CHARACTERIZATION AND RAPAMYCIN TREATMENT OF LARYNGOTRACHEAL STENOSIS, *IN VITRO* AND *IN VIVO*

By

Garret Ma

A thesis submitted to Johns Hopkins University in conformity with the requirements for the degree of Master of Science & Engineering

Johns Hopkins University
Baltimore, Maryland

May, 2015

ABSTRACT

Laryngotracheal stenosis (LTS) is an unpredictable, dynamic fibrosis which results in pathologic tissue buildup in the larynx and trachea resulting in airway narrowing. LTS can be caused by prolonged intubation, local trauma, autoimmune disease, radiation exposure, or idiopathic reasons. In many cases, LTS causes significant morbidity by limiting one's ability to speak, swallow and breathe, and may even cause mortality; however to date, there is no definite treatment to cure LTS.

Defining the cellular metabolism and function of normal and LTS-derived laryngotracheal fibroblasts are unclear. Biopsies were obtained from eight patients undergoing operative procedures for LTS and biopsies were taken from both "normal" and "scar" segments of their trachea. Fibroblast and cancer lines were analyzed *in vitro*. Scar fibroblasts demonstrated increased proliferation rates, larger cellular area and increased collagen-1 expression compared to normal. Metabolically, scar fibroblasts reveal lower levels of oxidative phosphorylation and a higher ECAR/OCR ratio. Through a comparative analysis, scar fibroblasts exhibit a greater reliance on aerobic glycolysis. Scar fibroblasts proliferate considerably more than normal cells. Through a comparative analysis, we were able to determine that scar fibroblasts exhibit many of the characteristics of the Warburg effect. We believe that this discovery may open promising opportunities to exploit this phenomenon and prevent the proliferation of LTS in patients.

Rapamycin was evaluated as a method to suppress proliferation and metabolism of scar fibroblasts *in vitro*. Rapamycin demonstrated an anti-fibrotic effect by reducing the

proliferation, metabolism, and collagen deposition of human LTS fibroblast *in vitro*. The bioenergetic effects of rapamycin demonstrated a significant decrease in oxidative phosphorylation of LTS fibroblasts, suggesting a potential mechanism for the reduction of proliferation and differentiation. Rapamycin's anti-fibrotic effects suggest a promising adjuvant therapy for the treatment of laryngotracheal stenosis. In addition, rapamycin when administered systemically *in vivo* when compared to PBS and dexamethasone, demonstrated a decrease in lamina propria thickness, a sign of decreased LTS. We believe that this one day could be translated to human clinical studies in order to provide a definitive treatment to a disease that currently has no effective therapy.

Advisors: Jennifer Elisseeff, Ph.D. & Alexander Hillel, M.D.

Reader: Kevin Yarema, Ph.D.

ACKNOWLEDGEMENTS

First and foremost, I would like to sincerely thank my two advisors, Jennifer Elisseeff and Alexander Hillel for giving me the opportunity to conduct science in their labs. Beyond that I cherish their mentorship and guidance throughout my progression these past two years. These insights will resonate and inspire me to achieve more and think further.

I would also like to thank the entirety of the Hillel and Elisseeff labs. Each and every person has contributed to my growth as an engineer and scientist by encouraging me to rationalize my choices, consider other options and find better more effective methods to tackle every problem. In particular, I would like to thank Daryan Namba and Idris Samad for working alongside me. They were critical bouncing board to evaluate the meaning of our results and it was a pleasure to collaborate with the two.

I have met many wonderful people outside of lab as one. Erin Zheng in particular has been a cornerstone to my success at Johns Hopkins. Her caring nature, indispensable support and everlasting ambition have been an inspiration for me.

Last but certainly not least, I am truly thankful for the support of my parents, Wen and Manny Ma. They have shown and guided me throughout my life. Their love and support are unwavering, unfiltered and continues to encourage me to this day. I am appreciative of their time and effort to make me a better individual. They always believe in me and

encourage me to take risk. Without their kind words of encouragement, life would not be as simple.

TABLE OF CONTENTS

LIST OF TABLES

LIST OF FIGURES

CHAPTER 1 – INTRODUCTION

1.1 Laryngotracheal Stenosis

Laryngotracheal stenosis (LTS) is a condition that is caused by pathologic fibrotic tissue buildup resulting in airway narrowing (**Figure 1**). LTS has numerous causes including, prolonged intubation, trauma, autoimmune disease, radiation, and idiopathic reasons. [1] [2] [3] Furthermore, it has been hypothesized that LTS may be the result of sustained inflammation that is caused by an abnormal increase in fibroblasts proliferation, collagen deposition, and subsequent scar tissue formation. [4] This disease has implications on breathing, speech and swallowing, in addition to a significant increase in morbidity and greater socioeconomic effects, due to prohibitive treatment costs and social effects of the disease. [5] [6] [7] Furthermore, LTS has the potential to progress to a stage where a patient may completely loses their airway, and may require an emergency tracheostomy, or other highly invasive surgical procedures. In some more extreme instances, LTS may even result in mortality.

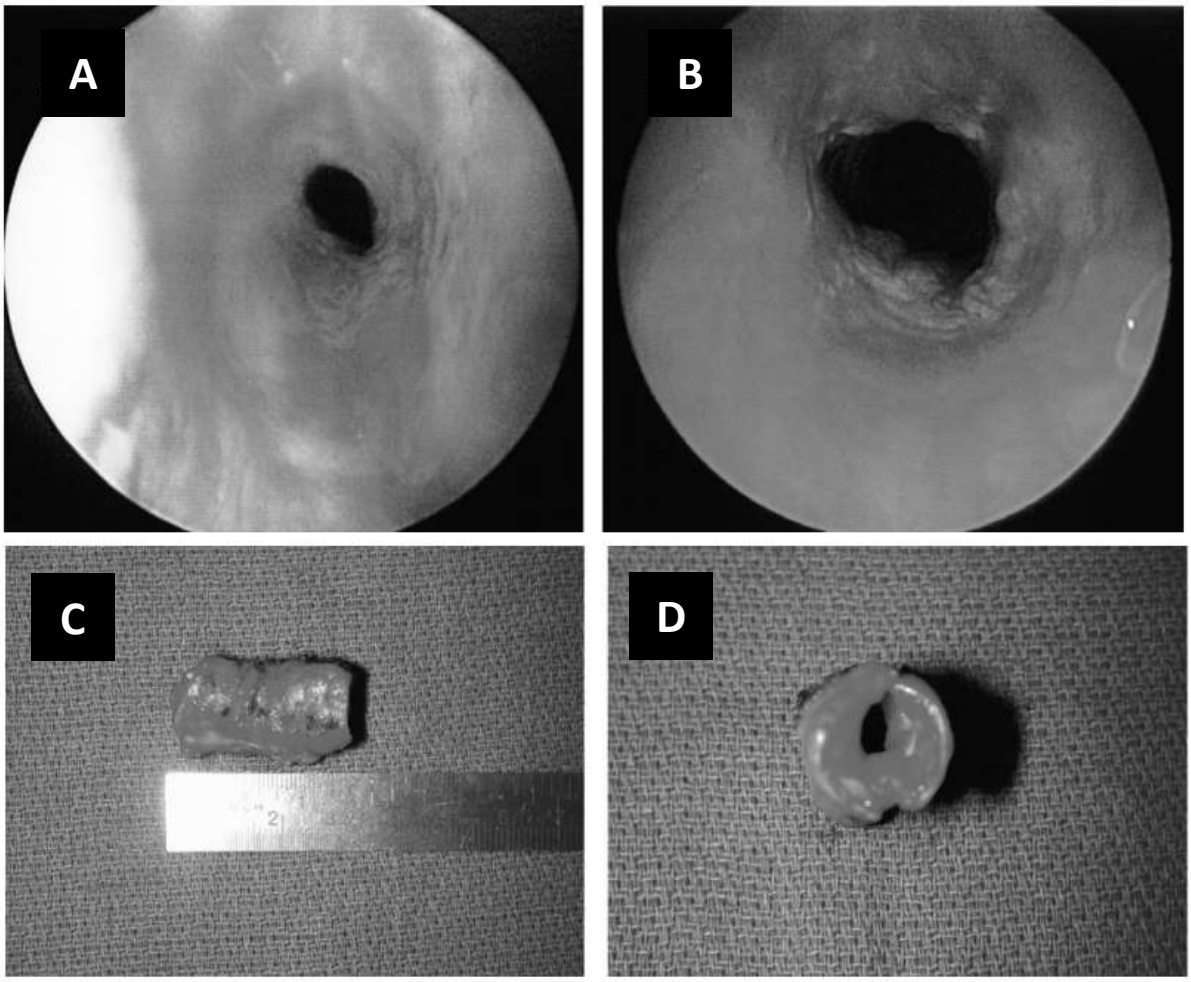

Figure 1 – Airways compromised by Laryngotracheal stenosis

(A) Constricted airway due to Laryngotracheal stenosis prior to dilation (B) Tracheal airway opened up post-dilation procedure (C & D) Cricotracheal resection specimen demonstrating LTS [1]

1.2 Current Therapies and Challenges

Current methods to combat LTS attempt to bypass the stenosis physically by opening the narrowed trachea via invasive surgical procedures including tracheostomy, stents, endoscopic scar excision and dilation, and tracheal & cricotracheal resection. [8] [9] [10] In conjunction with these procedures, local and systemic steroids and drugs such as mitomycin C, antibiotics and anti-inflammatory agents, have been used to slow the rate of scar formation. [5] [11] [12] [13] [14] [15] [16] [17] [18] The mechanism which these poorly understand therapies work and it should be noted these only serve as a temporary means to slow progression and do not treat LTS themselves. More fundamental and perhaps even more critical, is the lack of understanding between fibrotic and normal laryngotracheal tissue – notably fibroblasts – beyond physiological differences.

1.3 Rapamycin

Rapamycin (LC Labs, Woburn, MA) also known as sirolimus, rapamine is a macrocyclic antibiotic produced by the bacteria *streptomyces hygroscopicus*, that functions as an immunosuppressive medication. Rapamycin complexes with another protein to inhibit the mammalian Target of Rapamycin and prevents activation of lymphocytes and other immune cells, thereby inhibiting the normal immune response. [19] [20] [21] It is a Food and Drug Administration (FDA) approved drug that is frequently used as an antirejection agent for transplants well as in coronary stents to reduce restenosis and accelerated arteriopathy. [22] [23] [24] There is also evidence to suggest that rapamycin is effective in reducing fibrosis and proliferation in a variety of different cell tissue types including dermal, hepatic, and renal fibroblasts. [25] [26] [27]

1.4 Dexamethasone

Dexamethasone (Sigma-Aldrich, St. Louis, MO) is a corticosteroid that is commonly used as an anti-fibrotic agent to prevent the spread of fibrosis throughout the body including the airway and liver. [28] [29] [30] In the trachea, dexamethasone has been used to treat patients with LTS with significant success. [31] Given the positive results from dexamethasone, it serves as a strong positive control for *in vivo* experiments when comparing the results of rapamycin.

1.5 Fibrosis

Tissue injury can result in acute and chronic inflammation which, if expressed over a long period of time, can trigger fibrosis. Fibrosis is a dynamic disease process by which fibroblast dysfunction, on a cellular level, can eventually lead to organ dysfunction and clinical disease. This disease is not limited to a single organ, but can manifest throughout parts of the body, most commonly leading to the development of pulmonary fibrosis, cardiac fibrosis, or cirrhosis. Regardless of which organ is affected, untreated fibrosis will eventually lead to organ failure and possibly death. [32]

CHAPTER 2 – VARIATIONS IN NORMAL VERSUS FIBROTIC HUMAN LARYNGOTRACHEAL DERIVED FIBROBLASTS

2.1 Introduction

The objective of this study is to investigate the variability between fibrotic and normal fibroblasts *in vitro*. Determining the fibroblast's proliferative rates is critical to understanding ways to limit stenosis spread; genetic profiling provides a functional difference between the fibroblast types; histo-stereometric measurements provide physiological characteristics; while metabolic analysis helps better understand reasons behind the abnormal spread of LTS.

2.2 Materials and Methods

2.2.1 Fibroblast Isolation and Culture

After obtaining approval from the Johns Hopkins University Institutional Review Board, biopsies were obtained from eight patients undergoing operative procedures for LTS between 2012 and 2015. Informed consent was obtained prior to operation and biopsies were taken from both "normal" and "scar" segments of their subglottic trachea. Immediately after excision, tissue samples were placed in phosphate buffered saline (PBS; Gibco, Grand Island, NY) supplemented with 5% penicillin/streptomycin (Gibco). Biopsy specimens were then minced to ~1 mm^3 size pieces using a #10 Feather disposable scalpel (Graham-Field, Atlanta, GA), cut into a 100 x 20 mm uncoated tissue culture plastic petri dishes (Falcon by Corning, Corning, NY) and were grown in fibroblast growth medium at 37°C in 5% CO_2 humidified atmosphere. The fibroblast growth medium consists of Dulbecco's modified Eagle's medium (Gibco) supplemented with 10% fetal bovine serum (Thermo Scientific, Logan, UT), 100U/mL penicillin (Gibco),

100ug/mL streptomycin (Gibco), and 1X non-essential amino acids (Gibco). Once cells reached confluence, 0.25% Trypsin-EDTA treatment (Gibco) allowed fibroblasts to lift from the dishes, at which point cells were re-seeded onto tissue culture plastic flasks (BD Biosciences, San Jose, CA) for further expansion. Passage two or three of primary fibroblast cell lines were used for all experiments. Besides the cellular proliferation studies, cells were harvested on day six for the DNA assay, histological staining and PCR whereas cells were harvested on day two for the metabolic studies. Unless otherwise noted, cells were seeded at $5x10^3$ cells per well of a 6-well plate (BD Bioscience, Franklin Lakes, NJ).

JHU-011 cell line was obtained from the Division of Head and Neck Cancer Research, Johns Hopkins University in Baltimore, Maryland and was expanded from a laryngeal head and neck squamous cell carcinoma (HNSCC). [33] These cells were utilized for metabolic studies because they best exemplified laryngeal cancer of the head and neck. However, these cells had high adhesion to tissue culture plastic and were not suitable for cell proliferation studies.

HT-1080 cell line is a fibrosarcoma that was developed by American Type Culture Collection (Manassas, VA). These cells were used for cell proliferation, PCR and metabolic studies.

2.2.2 Cell Proliferation by Cell Count and DNA Assay

Once the fibroblast cells and the fibrosarcoma at confluence, they were trypsinized and seeded. Cell counts for the respective days were performed in duplicate using a hemocytometer.

Cells were enzymatically lysed and DNA assay was performed by fluorescently tagging cells using PicoGreen and analyzing them in duplicate per manufacturer's protocol (Invitrogen, Waltham, MA) [34]. The subsequent fluorescence was analyzed with a Synergy 2 Microplate Reader (BioTek Instruments, Winooski, VT).

2.2.3 Cellular Histology and Trichrome Staining

Fibroblasts were grown on microscope cover glass slips (Fisher Scientific, Hampton, NH) pretreated with 0.01% gelatin solution. The cells were stained with Masson's Trichrome #HT15 kit (Sigma-Aldrich, St. Louis, MO) in order to visually assess differences in collagen deposition between normal and scar fibroblasts. Cover slips with cells were dehydrated and mounted onto *Superfrost Plus* microscope slides (Fisher Scientific, Hampton, NH). Microscopic images of stained coverslips were viewed and captured using a Zeiss AX10 microscope (Carl Zeiss, Oberkochen, Germany). Stereological cellular area measurements were obtained using ImageJ (National Institute of Health, Bethesda, MD) in conjunction with a Wacom Tablet (Wacom, Kazo, Japan). [35] This experiment was run in triplicate per biological replicate.

2.2.4 Gene Expression Analysis by Real-Time Polymerase Chain Reaction

Fibroblasts and the fibrosarcoma were seeded in 6-well plates (BD Biosciences) at a concentration of $20x10^3$ cells per well, and were grown for six days. Cells were then harvested and frozen at -80 °C and the RNA was extracted using the RNeasy Micro Kit (Qiagen, Valencia, CA). Quantification of the RNA was accomplished using the nanodrop 2000 spectrophotometer (Thermo Scientific, Waltham, MA). cDNA synthesis was done using the iScript cDNA synthesis kit (BioRad, Hercules, CA). Quantitative Real Time PCR (qRT-PCR) was performed using the SYBR Green PCR Mastermix (Life Tech, Carlsbad, CA) on the StepOnePlus Real Time PCR System (Life Tech). Reaction mixtures were incubated for 10 min at 95°C followed by 40 cycles of 15s at 95°C, 1 min at 60°C, and finally 15s at 95°C, 1 min at 60°C, and 15s at 95°C. Collagen I was used as the target gene and Beta Actin (ACTB) as PCR control. The level of expression of the target gene was calculated as $2^{-\Delta\Delta Ct}$ equaling a fold change from each sample compared to each patient sets' respective "normal" fibroblast fold change. When assessing fibrosarcoma cells, the cancer cells were compared to an average of all patient sets' "normal" fibroblast fold change. This experiment was run in triplicate.

2.2.5 Cellular Oxygen Consumption Rate

Functional mitochondrial were analyzed by evaluating the oxygen consumption rate (OCR) via a XF24 Flux Analyzer and XF Cell Mito Stress Test (Seahorse Bioscience, Billerica, MA). Fibroblasts and the HNSCC were seeded in DMEM at $3x10^4$ cells/well a day prior to analysis. During the day of the mitochondrial stress test, the previous media was washed twice and exchanged with minimal XF Assay media supplemented with 25

mM glucose (Sigma-Aldrich, St. Louis, MO), 1X GlutaMax (Invitrogen, Waltham, Massachusetts) and 1X Non-Essential Amino Acids (Invitrogen, Waltham, Massachusetts) per the manufacturer's protocol. The cells were allowed to acclimate for an hour at 37°C in a humidified atmosphere without CO_2 prior to mitochondrial stress test. Oxygen consumption rates are determined by using 10 uM Oligomycin, an ATP Coupler, injected at 34 minutes, 4 uM Carbonyl cyanide-p-trifluoromethoxyphenylhydrazone, FCCP, an ATP uncoupler, injected at 72 minutes, 20 uM Rotenone and Antimycin, mitochondrial inhibitors, injected at 110 minutes. Through the metabolic stress test, the Basal Metabolic rate, ATP production and maximal respiratory capacity can be elucidated. To ensure that post stress test the number of cells had remained the same, a PicoGreen DNA was used to determine that the total protein amount to be roughly 10mg per well.

2.2.6 Cellular Extracellular Acidification Rates

Glycolytic function measurements were analyzed by evaluating the Extracellular Acidification Rate (ECAR) using a XF24 Flux Analyzer. The fibroblasts and the HNSCC were seeded in DMEM at $4x10^4$ cells/well a day prior to analysis. During the day of the glycolytic stress test, the previous media was washed twice and exchanged with minimal XF Base glucose-free media without supplements per the manufacturer's protocol. The cells were allowed to acclimate for an hour at 37°C in a humidified atmosphere without CO_2 prior to mitochondrial stress test. Oxygen consumption rates was determined by using 5 mM Glucose, a glycolysis substrate, injected at 34 minutes, 10 uM Oligomycin, a ATP Synthase Inhibitor, injected at 72 minutes, 2 uM 2-Deoxy-D-

glucose, a Glycolysis Inhibitor, injected at 110 minutes. Similarly to the oxidative phosphorylation test, PicoGreen was used to verify DNA concentration.

2.2.7 Statistical Analysis

Results are expressed as averages ± standard error of the mean. For cellular area, a Mann-Whitney Test and p-value < 0.05 is considered significant. For proliferation, DNA assay, metabolic studies, a Wilcox Signed Rank Test and p-values < 0.05 is considered significant. Statistics were conducted using Prism (GraphPad; La Jolla, California).

2.3 Results

2.3.1 Scar fibroblasts showed increased cell proliferation when compared to normal

When cultured and grown under the same conditions in vitro, scar fibroblasts demonstrate an increased cell proliferation rate verified through cell counting measurements and DNA assay measurements across all five of our patient cell lines (**Figure 2A**). However, both fibroblast cell types grew a far slower rates in comparison to the fibrosarcoma (**Figure 2B**). Furthermore, when analyzing the DNA per cell ratio on average for normal and scar were not significantly different at 25.87 ± 16.79 pg/cell and 46.15 ± 44.39 pg/cell, respectively (p-value = 0.2317). In contrast, the fibrosarcoma had 16.00 pg/cell.

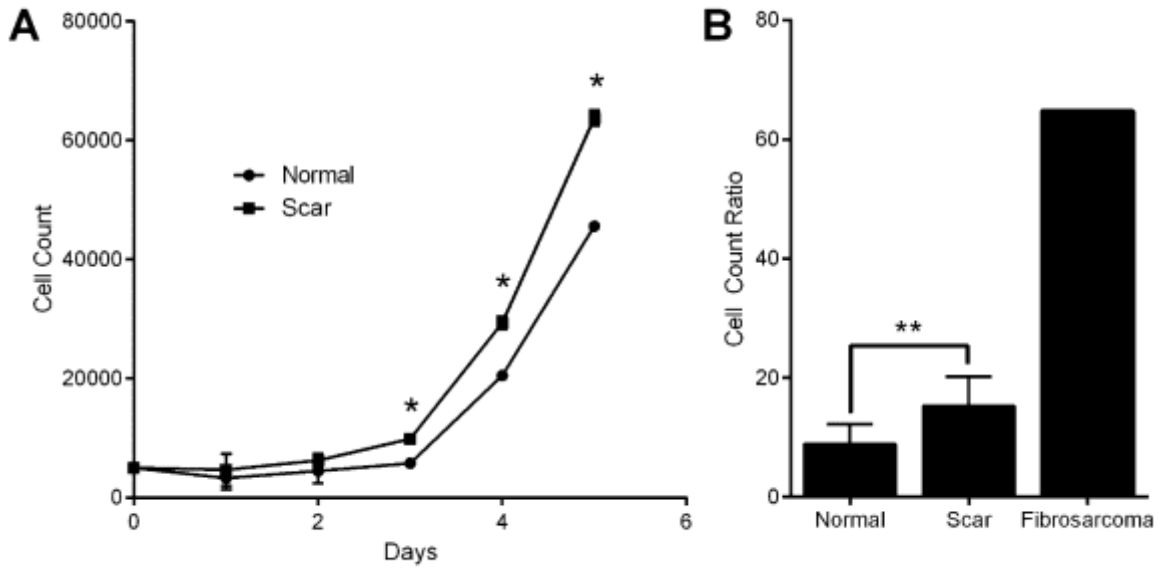

Figure 2 - Scar fibroblasts proliferate more than normal fibroblasts

(A) This figure demonstrates a typical patient set. Although from the initial seeding until day 2 there are no significance, the last three days of the study, proliferation has resulted in a significant difference of $p = 0.002$, $p = 0.0003$, $p < 0.0001$ for days three, four, and five, respectively, between normal and scar cell lines (B) Cell count growth ratio between day five and the initial seeding

2.3.2 Similar Stereometric Measurements verified via Cellular Histology and Trichrome Staining

Scar fibroblasts demonstrate increased cell proliferation compared to normal fibroblasts when assessing using microscopy after staining with Masson's Trichrome to visualize cells (**Figure 3**). Morphology of both normal and scar fibroblasts appears similar with no significant differences seen in average cell length. On average, normal and scar cells measured 1164.70 ± 995.41 μm2 and 1549.69 ± 976.21 μm2, respectively (p-value = 0.0167).

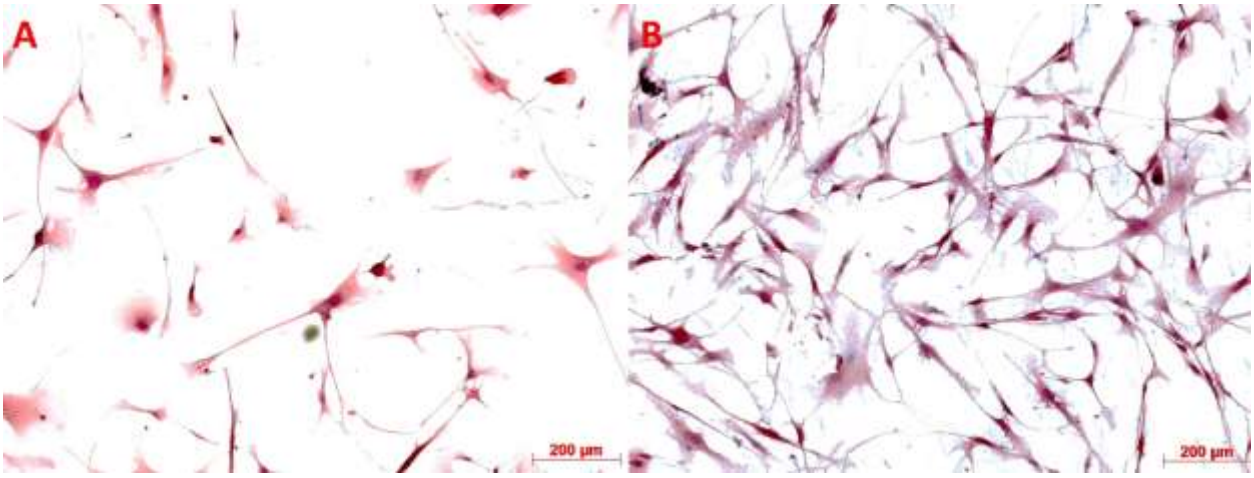

Figure 3 - Morphological and proliferative differences

Normal (A) and Scar (B) were imagined at Day 6 at 10x Magnification. Scar cells demonstrated an increased proliferation and cellular area when compared to Normal cells, both of which are captured in the figure.

2.3.3 Collagen Gene Expression elevated in Scar Fibroblasts

In comparison to normal laryngotracheal fibroblasts, scar fibroblasts demonstrate increased collagen gene expression (**Figure 4**) (p-value = 0.0391). Nevertheless the two show far lower than the fibrosarcoma gene expression for Collagen I.

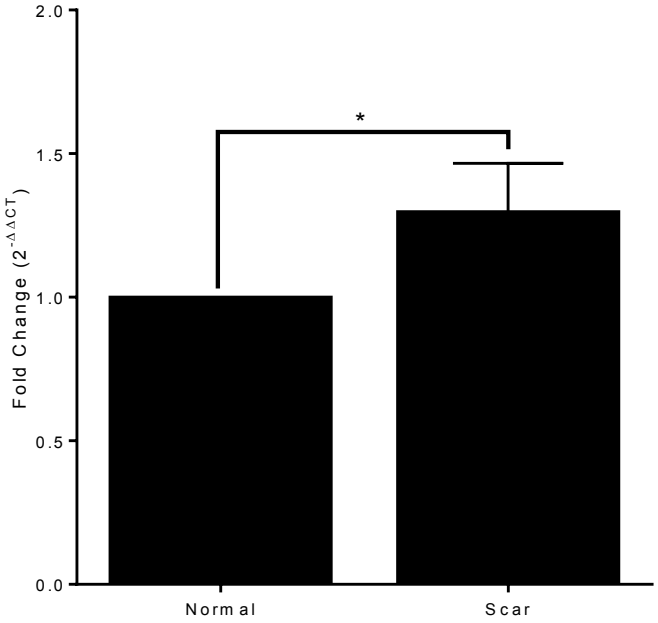

Figure 4 - Collagen 1 Expression Greater in Scar Fibroblasts

When normalized to respective Patient Set Normal Laryngotracheal Fibroblasts, Scar Fibroblasts express higher Collagen 1 fold change in comparison to Normal Fibroblasts.

2.3.4 Cell Oxidative Phosphorylation

Normal laryngotracheal fibroblasts were more metabolically active in oxidative phosphorylation than scar laryngotracheal fibroblasts. Basal metabolism, ATP production and maximal respiratory capacity, were significantly different in normal fibroblasts than in scar fibroblasts and were elevated when compared to HNSCC (**Figure 5A, 5B, 5C**). **Figure 5D** shows a representative graph of a normal and scar mitochondrial stress test. Basal metabolism is calculated by taking the difference in the peak OCR prior to oligomycin and the base OCR after the rotenone & antimycin injection. ATP production is calculated by evaluating the difference pre and post oligomycin injection. Maximal respiratory capacity was determined by the difference between the peak OCR post-FCCP injection and the base OCR post rotenone & antimycin injection.

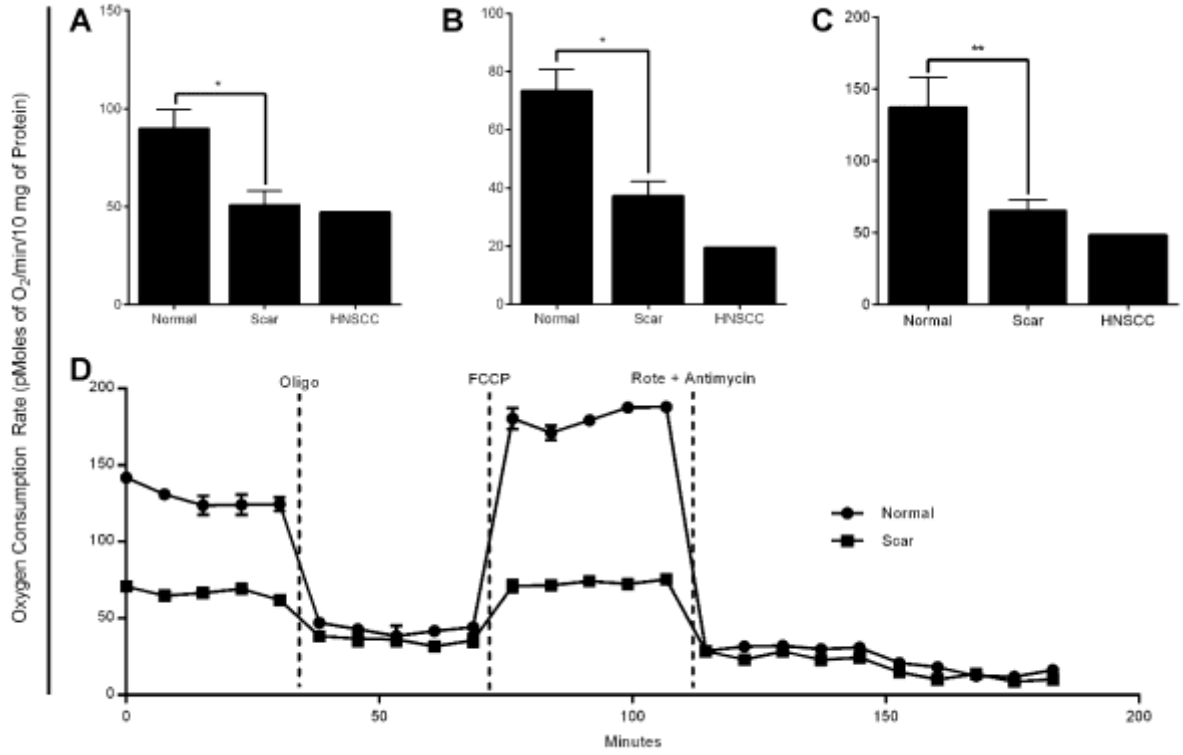

Figure 5 - Increased Oxidative Phosphorylation Capacity in Normal Fibroblasts

Normal fibroblasts show a significant difference in (A) Basal Respiration, (B) ATP Production and (C) Maximum Respiration at $p = 0.0004$, $p = 0.0003$, $p < 0.0001$, respectively. Panel (D) demonstrates a Mitochondrial Stress Test of a patient set conducted in a XF24 Analyzer.

2.3.5 Cell Extracellular Acidification

Normal and Scar fibroblasts demonstrated no significant difference in glycolytic capacity (**Figures 6A**). The difference between the peak ECAR post oligomycin and the base ECAR value post 2-DG is used to calculate the glycolytic capacity. Figure 6C demonstrates a typical normal and scar glycolytic stress test chart. Furthermore, by taking the ratio of glycolytic capacity to maximum respiration from Figure 4, the cellular dedication to either metabolic pathway can be elucidated for each cell type (**Figure 6B**). HNSCC demonstrated greater ECAR/OCR than scar but both showed a greater preference to aerobic glycolysis than normal fibroblasts.

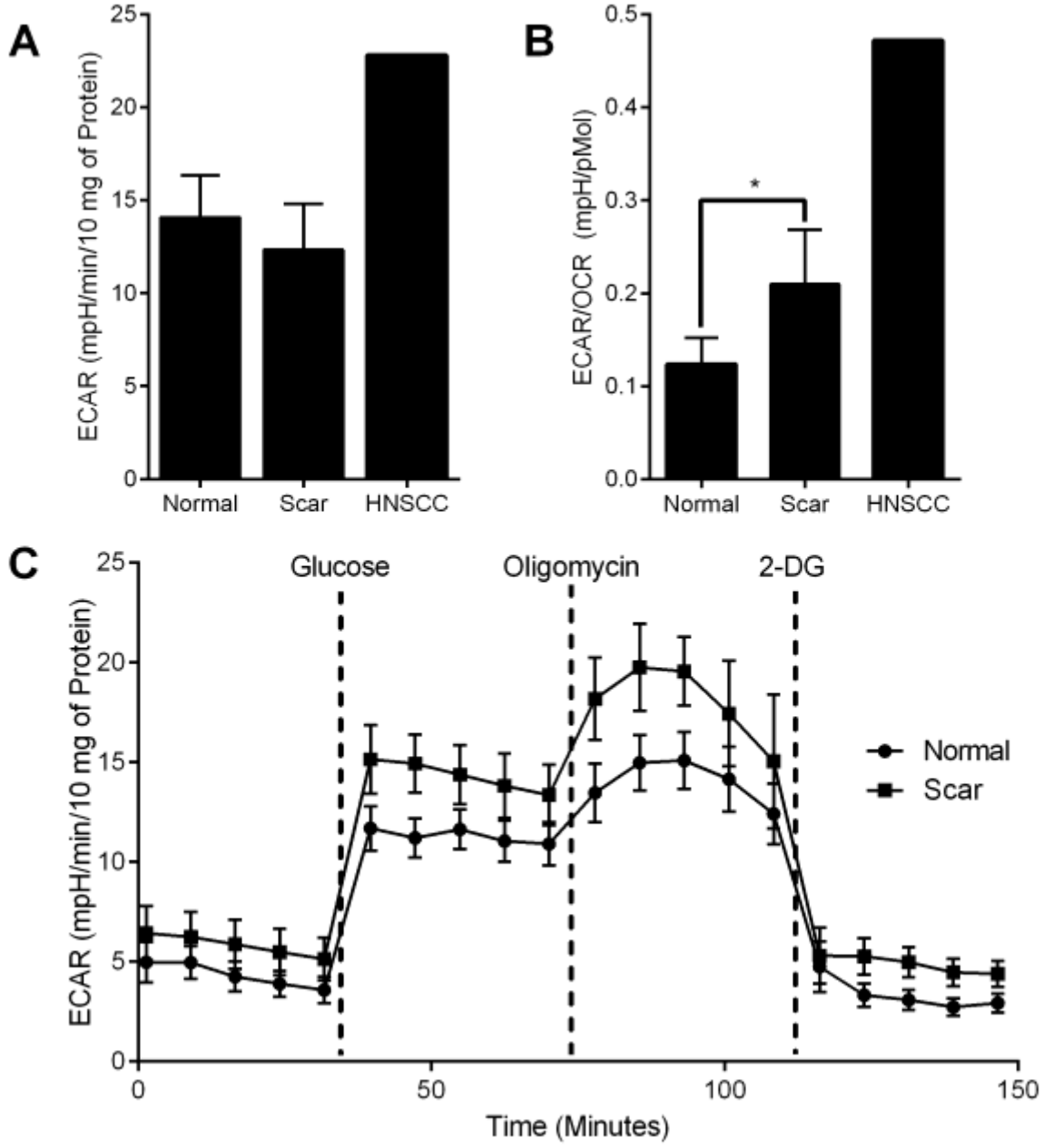

Figure 6 - Metabolic Glycolysis Dedication

Normal and Scar Fibroblasts are similar in (A) Glycolytic Capacity, (B) ECAR/OCR Ratio. Panel (C) demonstrates a Glycolytic Test conducted on an XF24 Analyzer of a patient set.

2.4 Discussion

The analysis of normal and scar laryngotracheal fibroblasts illustrate proliferative, gene expression and metabolism provides a more targeted approach to finding a sustainable treatment for LTS. In the eight patients cells used in this study as well as the cancer lines, we see that scar fibroblasts proliferate at a significantly faster rate when compared to normal fibroblasts, which accounts for the stenosis spread seen in typical LTS patients. Nevertheless, both were draft by the proliferative ability of the fibrosarcoma. These results are mirrored on a genetic level; scar fibroblasts express and deposit collagen at a rate that mirrors clinical effects of collagen deposition at the site of stenosis. [26] [36] More surprising was, when analyzing the metabolic differences between normal and scar fibroblasts, normal fibroblasts demonstrated, on a bioenergetics level, higher mitochondrial metabolism and similar levels of aerobic glycolysis which mirrors “the Warburg effect”.

The biological phenomenon termed as the “the Warburg effect” is the observation that cells predominantly plant and cancer cells rely primarily on aerobic glycolysis rather than oxidative phosphorylation which results in larger lactic acid buildup. [37] [38] However, although there is a greater reliance on aerobic glycolysis, mitochondrial oxidative phosphorylation seems to remains functional. [39] Albeit cancer or scar cells, the reason behind why cells seem to rely on the “Warburg effect” rather than on the more efficient oxidative phosphorylation is not clearly understood.

Oxidative Phosphorylation and glycolytic analysis allows us to determine the bioenergetic levels on the cellular level. [40] [41] Our study demonstrates that normal fibroblasts consumed more oxygen than scar fibroblasts and HNSCC when concerning basal metabolism, ATP production and maximal respiration (**Figure 5**). However when assessing glycolytic metabolism, both normal and scar fibroblasts demonstrate similar glycolytic capacity though the HNSCC demonstrated an elevated amount. Interestingly, when looking at the ratio between glycolytic capacity and maximal oxidative phosphorylation, scar cells demonstrate greater than two-fold increase compared to normal fibroblasts which was also demonstrated in the HNSCC (**Figure 6**). With this metabolic data in conjunction with the increased proliferative effects of scar fibroblasts in comparison to normal cells, scar cells seem to be undergoing a Warburg-like effect.

It is important to note the limitations of the *in vitro* study on normal human laryngotracheal and scar fibroblasts. *In vitro* studies are not representative or indicative of fibroblasts *in vivo* but rather serves as a model to help bridge our understanding between the differences between the two cell types. In order to prevent changes to the primary harvested fibroblasts due to the *in vitro* environment, we limited the study to only passage two or three cells and restricted repeated passaging and freeze-thawing of the cells. Nevertheless, these may have had an effect on the cellular phenotype, genotype, and behavior. Furthermore, as with any primary harvested cells, there are variability between patients in which the cells were derived from. The effects of the variability was limited by conducting paired statistical analyses between normal and scar fibroblasts to decrease the effects of heterogeneity of the disease process.

Nevertheless, we are encouraged by the significant differences between normal and scar fibroblasts across the collective patient sets. Cancers cells were added to this study to provide a perspective that although normal and scar cells demonstrate statistically different features they still are starkly different from the fibrosarcoma and HNSCC on my fronts. But more importantly, it demonstrates that scar fibroblasts Warburg-like effects though deeper analysis is necessary to determine whether or not the cells truly are under the influence of the Warburg effect. Additional studies on the genetic level and metabolic studies comparing anaerobic and aerobic glycolysis will be needed.

In conclusion, normal and scar fibroblasts show similarities and differences when considering proliferation, histo-stereology, genetic variability, and metabolism *in vitro*. By exploiting these differences while keeping in mind their similarities, stenosis and scar formation can be targeted more effectively. Furthermore, the Warburg-like effect between scar fibroblasts and cancer cells tested shows promise that this may be an unexplored avenue to the treatment of laryngotracheal stenosis.

CHAPTER 3 – RAPAMYCIN INHIBITS HUMAN LARYNGOTRACHEAL STENOSIS DERIVED FIBROBLAST METABOLISM *IN VITRO*[1]

[1] Permission to reproduce *Rapamycin Inhibits Human Laryngotracheal Stenosis–derived Fibroblast Proliferation, Metabolism, and Function in Vitro* published in *American Academy of Otolaryngology – Head and Neck Surgery* was received by Alexander Hillel, Garret Ma, Idris Samad, and Daryan Namba on March 11, 2015. Per the Transfer of Copyright Agreement from the publisher, authors reserve the right to "include the article in full or in part in a thesis or dissertation"

3.1 Introduction

The aim of this study was to determine whether rapamycin could inhibit human LTS fibroblast proliferation *in vitro*. Fibroblast proliferation is a crucial step for development of LTS and collagen is usually implicated in deposition of scar tissue and in fibrosis. Therefore, we hypothesized that rapamycin would decrease LTS fibroblast proliferation and metabolism, and reduce collagen production. We characterized the effect of rapamycin on fibroblasts through growth kinetics, morphology, gene expression, and cellular metabolism profile.

3.2 Materials and Methods

3.2.1 Laryngotracheal Fibroblast Isolation and Culture

Biopsy of human laryngotracheal stenosis was performed during routine suspension microlaryngoscopy, bronchoscopy, excision and dilation of subglottic/tracheal stenosis in 5 patients. Informed consent was obtained from all patients to join this study, which was approved by the Johns Hopkins Institutional Review Board (NA_00078310). Immediately after excision, tissue samples were placed in phosphate buffered saline (PBS; Gibco Life Technologies by Invitrogen, Grand Island, NY) supplemented with 5% penicillin/streptomycin (Gibco). Biopsy specimens were minced and the tissue fragments were spread out evenly across uncoated plastic tissue culture flasks (BD Biosciences, San Jose, CA) and suspended in fibroblast growth medium at 37°C in 5% CO2-humidified atmosphere. Fibroblast growth medium consisted of Dulbecco's modified Eagle's medium (DMEM; Gibco) supplemented with 10% fetal bovine serum

(FBS; HyClone by Thermo Scientific, Logan, UT), 100U/mL penicillin (Gibco), 100ug/mL streptomycin (Gibco), and 100x non-essential amino acids (NEAA; Gibco). Once cells were confluent (between 20-30 days) short-term 0.25% Trypsin-EDTA treatment (Gibco) proved effective in releasing only fibroblasts from the flasks, which were then plated into new flasks for expansion. Passage two or three of these primary fibroblast cell lines were used in the following experiments. To confirm culture of fibroblasts, cells were analyzed to be pan cytokeratin negative as well as Mason's Trichrome stain positive. The former of which were compared against known fibroblasts (CRL 2522) and fibrosarcoma (HT 1080).

3.2.2 Cell Proliferation by Cell Count and DNA Assay

After reaching confluence, the adherent LTS fibroblasts were trypsinized and passaged into 12-well culture plates (Falcon by BD Biosciences) containing fibroblast growth medium, and seeded with 20,000 cells per well. Medium was aspirated and replaced daily with the following conditions: 1) control, normal fibroblast growth medium; 2) control-vehicle, medium containing vehicle solution, 1% dimethyl sulfoxide (DMSO); 3) rapamycin-1, medium containing rapamycin (Sigma-Aldrich, St. Louis, MO) dissolved in DMSO at a concentration of 1ng/mL or 10^{-10} M; 4) rapamycin-10, medium containing rapamycin dissolved in DMSO at a concentration of 10ng/mL or 10^{-9} M. These concentrations were chosen based on previous literature (Poulahan 28, Milani). All conditions were grown in triplicate. Cells were harvested on the 6th day of incubation and the trypsinized LTS fibroblasts were counted in duplicate. Following, the LTS fibroblasts of each well were lysed (10 mM Tris, 1 mM EDTA, 0.1% Triton X-100 and

0.1 mg/ml Proteinase K) and DNA concentration was determined using the PicoGreen fluorescent method, adapted from the manufacturer's protocol (Invitrogen Quant-iT PicoGreen dsDNA Reagent and Kits Protocol, Molecular Probes P11496). [42] Each sample was run in duplicate for the assay. Fluorescence was read using the BioTek Synergy 2 Microplate Reader (BioTek Instruments, Winooski, VT).

3.2.3 Gene Expression Analysis by Real Time Polymerase Chain Reaction

LTS fibroblasts were seeded in 6-well culture plates (Falcon by BD Biosciences) with 300,000 cells per well and grown in the four medium conditions in duplicate for 6 days. The RNeasy Micro Kit (Qiagen, Valencia, CA) was used for RNA extraction of each well and the RNA was quantitated using the nanodrop 2000 spectrophotometer (Thermo Scientific, Waltham, MA). The iScript^{TM} cDNA synthesis kit (BioRad, Hercules, CA) was used for cDNA synthesis according to the manufacturer's protocol. Quantitative Real Time PCR (qRT-PCR) was performed and monitored using the SYBR Green PCR Mastermix (Life Tech, Carlsbad, CA) on the StepOnePlus Real Time PCR System (Life Tech). Reaction mixtures were incubated for 10 min at 95°C followed by 40 cycles of 15 seconds at 95°C, one min at 60°C, and finally 15 seconds at 95°C, one min at 60°C, and 15 seconds at 95°C. For each sample, gene expression was corrected against Beta Actin level. All samples were run in duplicate. The level of expression of the target gene was calculated as $2^{\Delta\Delta Ct}$ as previously described. [43] The control LTS fibroblasts grown in normal growth medium were used for reference. Error was calculated by the standard deviation of ΔΔCT. [44] The fibrosis marker, Collagen I (Col I) was assessed as previously described. [45]

3.2.4 Cellular Metabolism using Oxygen Consumption Rate Measurements

Bioenergetic analysis of oxygen consumption rate (OCR) provides a measurement of overall metabolic status of the cell. [46] OCR measurements of LTS fibroblasts were completed using a Seahorse XF24 Flux Analyzer (Seahorse Bioscience, Billerica, MA) at $4x10^4$ cells per well. They were grown in the four medium conditions for two days post seeding with respective medium changed daily. The assay used XF minimal assay medium supplemented with 25mM glucose (Sigma), 1X GlutaMax (Invitrogen) and 1X Non-Essential Amino Acids (Invitrogen). Prior to the stress test, the cells were washed twice with this medium and incubated for one hour at 37°C in a humidified atmosphere without CO_2. In order to evaluate the mitochondrial respiratory capacity, Oligomycin (an ATP Coupler), Carbonyl cyanide-p-trifluoromethoxyphenylhydrazone (FCCP, an ATP uncoupler), Rotenone and Antimycin (mitochondrial inhibitors) at 10uM, 4uM and 20uM concentration, respectively, were injected into the medium at 34, 72, and 110 minutes respectively. PicoGreen DNA quantization assay was performed on each well in order to normalize the OCR. DNA content was correlated with the total protein amount per well. Basal metabolic rate, ATP production and maximal respiratory capacity were measured.

3.2.5 Statistical Analysis

Results were expressed as averages ± standard error of the mean. Wilcox Signed Rank Test and *p*-values < 0.05 were considered significant (STATA; StataCorp LP; College Station, Texas).

3.3 Results

3.3.1 Rapamycin decreases LTS fibroblast proliferation

Increased rapamycin dosing showed a decreased LTS fibroblast growth rate in all patients (**Figures 7A**, **8A**) as well as in the mean (**Figure 8B, 8B**) for all patients. Although in all medium conditions the fibroblasts grew, fibroblasts grown in normal medium conditions (mean = 21.9 x 10^4, STD = 3.9 x 10^4) grew at a faster rate than the fibroblasts grown in DMSO (mean = 17.9 x 10^4, STD = 5.0 x 10^4), low-dose (mean = 8.7 x 10^4, STD = 2.1 x 10^4) and high-dose Rapamycin (mean = 4.8 x 10^4, STD = 1.0 x 10^4, respectively). There was a significant decrease in individual (**Figure 7A**) and average (**Figure 7B**) LTS fibroblast count cultured with high-dose rapamycin versus DMSO vehicle control (p = 0.0007) and normal (p = 0.0007) medium. Low-dose rapamycin also demonstrated a significant reduction in fibroblast count when compared to control (p = 0.0008) and normal (p = 0.0007) medium. Of those same counted fibroblasts, there was a significant decrease in DNA concentration of individual (**Figure 8A**) and average (**Figure 8B**) LTS fibroblasts cultured with high-dose rapamycin versus DMSO vehicle control (p = 0.0007) and normal (p = 0.0007) medium. There was also a significant difference in DNA concentration for fibroblasts grown in low-dose rapamycin versus normal (p = 0.0026) and vehicle medium (p = 0.0015). DNA/cell was not significantly different from different cell medium types.

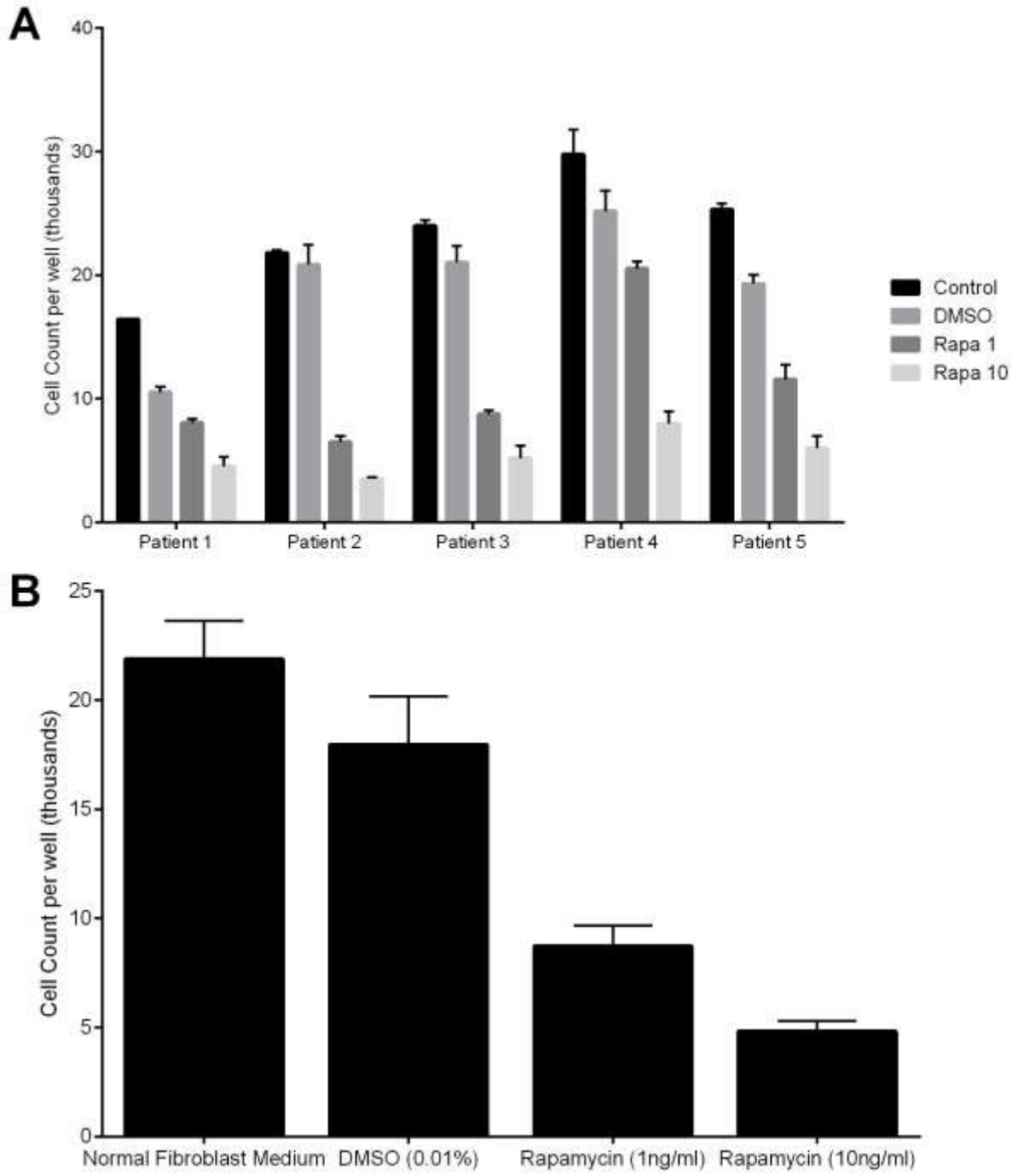
A
Cell Count per well (thousands)
40
30
20
10
0
Patient 1
Patient 2
Patient 3
Patient 4
Patient 5
Control
DMSO
Rapa 1
Rapa 10
B
Cell Count per well (thousands)
25
20
15
10
5
0
Normal Fibroblast Medium
DMSO (0.01%)
Rapamycin (1ng/ml)
Rapamycin (10ng/ml)

Figure 7 - Rapamycin reduces fibroblast count

Fibroblast count shows a significant reduction in proliferation of laryngotracheal stenosis-derived fibroblasts after treatment with low- and high-dose rapamycin in all 5 patients' cells (A) compared to normal medium and vehicle medium controls. Average cell count (B) shows significance when comparing low-dose Rapamycin compared to normal ($p = 0.0008$) and DMSO ($p = 0.0007$) controls. Similarly, at high-dose Rapamycin there was a significant difference compared to normal ($p = 0.0007$) and DMSO ($p = 0.0007$) controls.

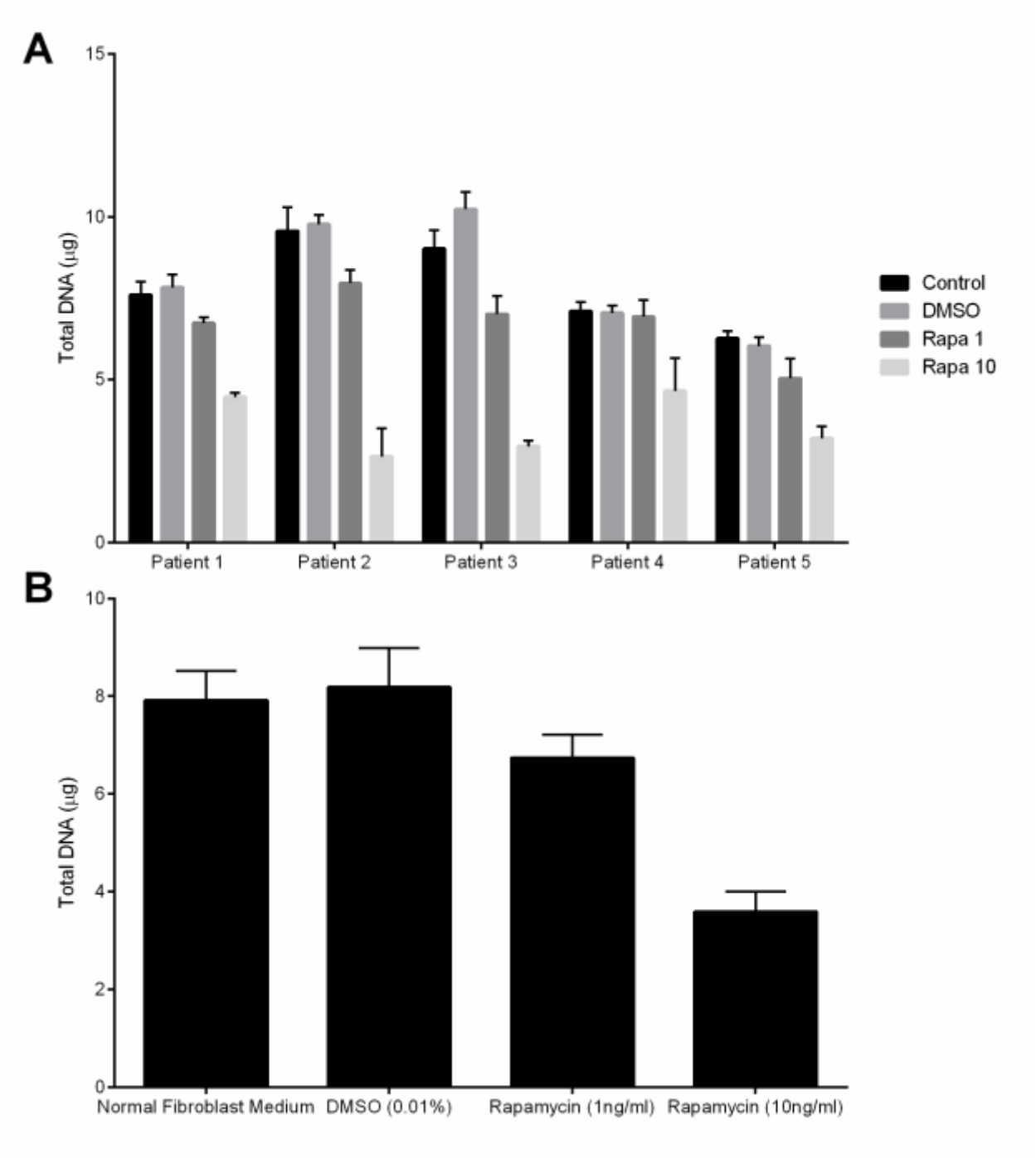
A
Total DNA (µg)
15
10
5
0
Patient 1
Patient 2
Patient 3
Patient 4
Patient 5
Control
DMSO
Rapa 1
Rapa 10
B
Total DNA (µg)
10
8
6
4
2
0
Normal Fibroblast Medium
DMSO (0.01%)
Rapamycin (1ng/ml)
Rapamycin (10ng/ml)

Figure 8 - Rapamycin significantly inhibits fibroblast proliferation

Cell proliferation, measured by DNA assay, demonstrates a significant reduction of laryngotracheal stenosis-derived fibroblast proliferation after treatment with low-dose rapamycin in all 5 patients' cells (A) compared to normal and vehicle controls. When patient results are averaged (B), fibroblast proliferation shows a reduction with high-dose rapamycin treatment compared to normal ($p=0.0007$) medium and DMSO-vehicle ($p=0.0007$) medium controls. Similarly, with low-dose rapamycin treatment, there was a significant difference when compared against normal ($p = 0.0036$) medium and DMSO-vehicle ($p = 0.0015$) medium controls.

3.3.2 Rapamycin treated fibroblasts demonstrate reduced collagen staining

LTS fibroblasts were stained with Masson's Trichrome in order to visualize collagen deposition, which stains blue. Histological evaluation of LTS cultured cells after treatment of rapamycin showed a decrease in collagen deposition compared to LTS cells untreated with rapamycin (**Figure 9**).

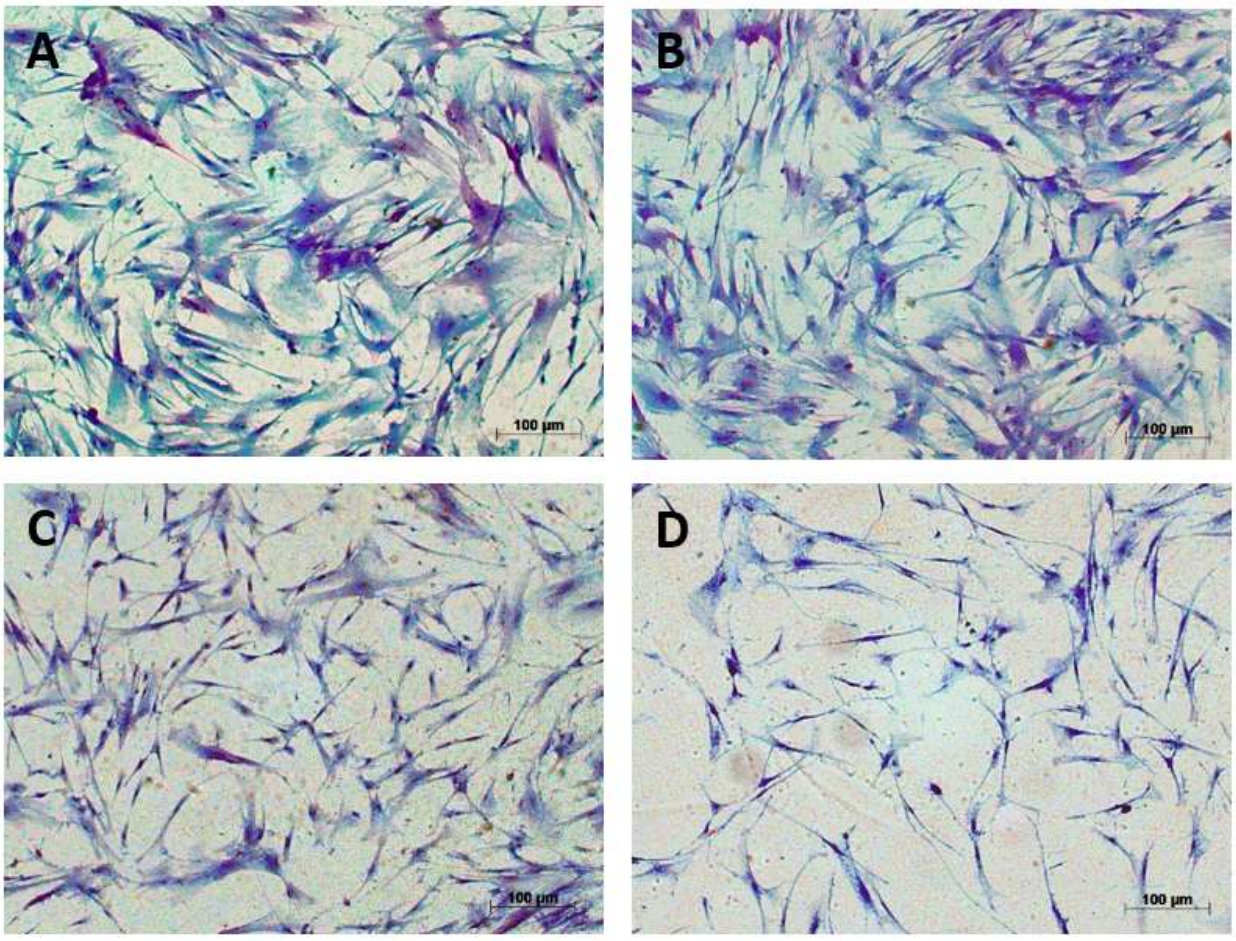

Figure 9 - Morphologic Staining of Drug-Induced Fibroblasts

Normal (A) and DMSO-vehicle (B) controls demonstrate confluent fibroblasts with intense blue staining for collagen by Masson's Trichrome. There is a reduction in fibroblast density and collagen deposition after treatment with low- (C) and high-dose (D) rapamycin. All cells grown for 5 days in their respective medium.

3.3.3 Rapamycin-treated Fibroblasts have reduced Collagen I Expression

RT-PCR demonstrated decreased collagen I gene expression in rapamycin treated LTS fibroblasts compared to control LTS fibroblasts in all five patients (**Figure 10A**). The average of all five patients also showed a linear trend in which increasing rapamycin concentration resulted in a decrease in collagen I gene expression (**Figure 10B**). There was a significant decrease in collagen I expression between LTS fibroblasts grown in high dose 10ng/mL rapamycin and in control fibroblast medium (p = 0.0051) and in DMSO vehicle medium (p = 0.0093). There was also a significant decrease in collagen I expression in LTS fibroblasts grown in low-dose rapamycin versus control (p = 0.0069) but not against the vehicle (p = 0.0745) medium.

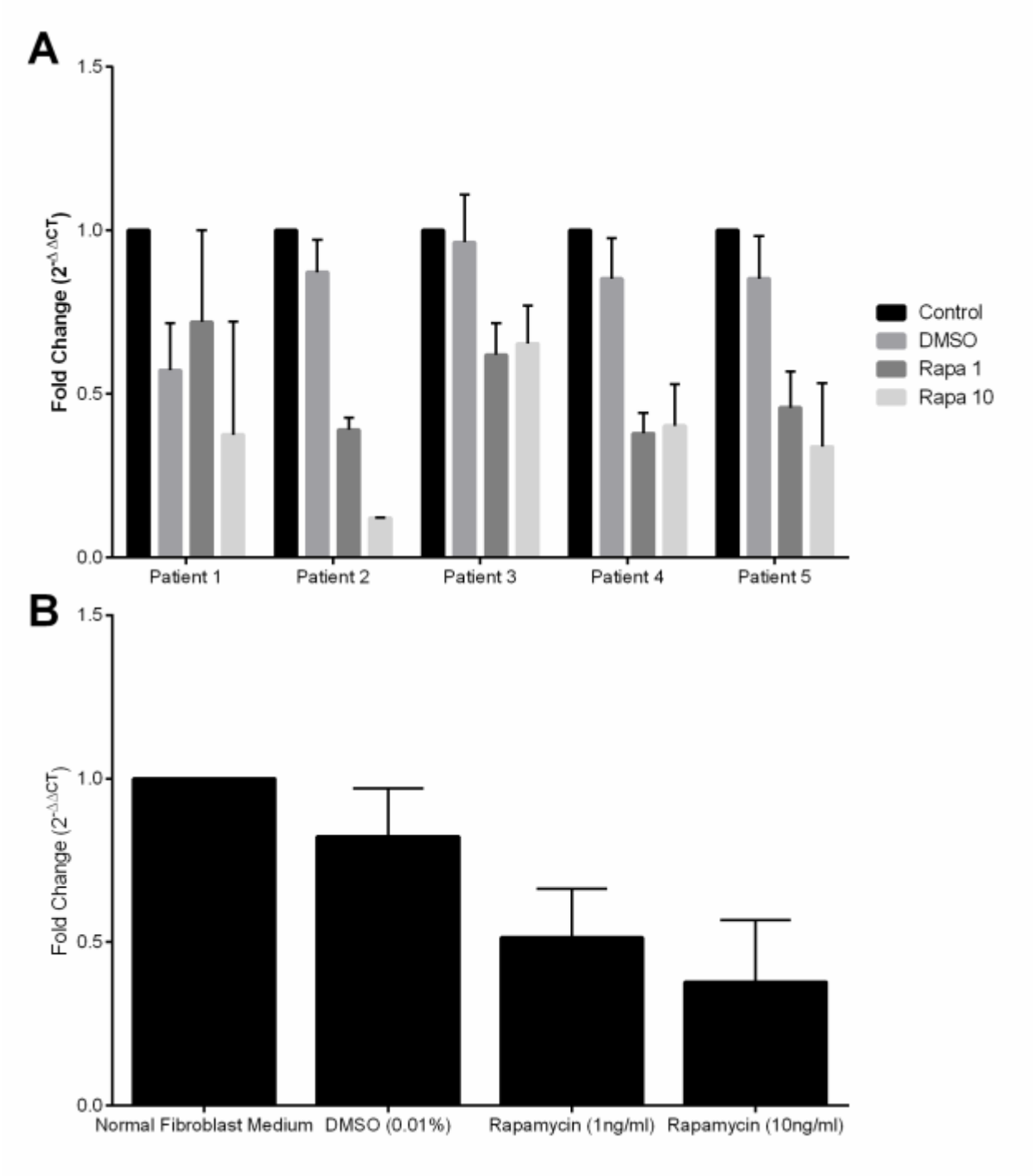
A
1.5
1.0
0.5
0.0
Fold Change (2^-ΔΔCT)
Patient 1
Patient 2
Patient 3
Patient 4
Patient 5
Control
DMSO
Rapa 1
Rapa 10
B
1.5
1.0
0.5
0.0
Fold Change (2^-ΔΔCT)
Normal Fibroblast Medium
DMSO (0.01%)
Rapamycin (1ng/ml)
Rapamycin (10ng/ml)

Figure 10 - Collagen 1 expression is inhibited by rapamycin

(A) Four of 5 patients demonstrate a significant reduction in Collagen 1 gene expression compared to normal medium and vehicle medium controls. (B) When averaged together, collagen 1 expression demonstrates a decreasing effect with increasing rapamycin dosing.

3.3.4 Rapamycin decreases the metabolic rate of LTS fibroblasts

LTS patient-derived fibroblasts were less metabolically active than those grown in normal and vehicle medium controls (**Figures 11A-D**). When averaged together, there were significant decreases in basal respiration (**Figure 17A**), ATP production (**Figure 17B**), and maximal respiration (**Figure 11C**) between LTS fibroblasts treated with high-dose rapamycin and those cultured in DMSO control ($p < 0.05$) and fibroblast growth medium ($p < 0.05$). **Figure 11D** demonstrates the difference in a representative patient's fibroblast oxygen consumption rate between the three medium conditions: normal medium control, DMSO control, and high-dose rapamycin. High-dose rapamycin decreased the basal metabolic rate (difference in peak OCR prior to Oligomycin and lowest OCR post Rotenone/Antimycin) and ATP production (difference in OCR prior to and post Oligomycin injection) and decreased maximal respiratory capacity (difference between peak OCR post-FCCP injection and the non-mitochondrial respiration) in LTS Fibroblasts.

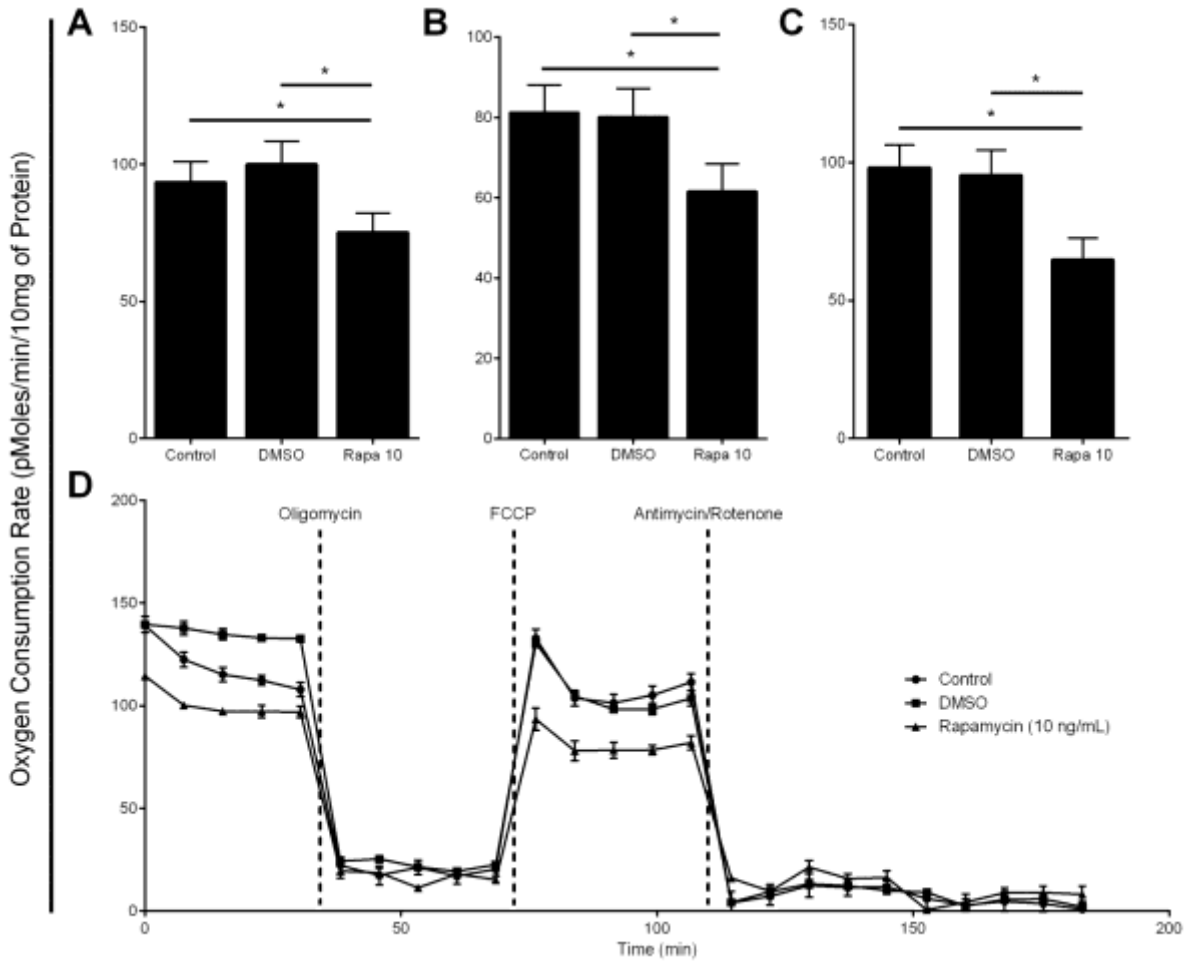

Figure 11 - Rapamycin decreases the metabolic rate of LTS fibroblasts

(A) Mean basal respiration, (B) ATP production, and (C) maximal respiration significantly decreased with high-dose rapamycin when compared to normal medium and vehicle medium controls. (D) Oxygen consumption rate in representative patient-derived fibroblasts. Fibroblast cells were seeded in XF96 V3-PS cell culture microplate (Seahorse Bioscience) in fibroblast growth medium (FGM), FGM+DMSO, and FGM+DMSO+rapamycin(10ng/mL) medium. ATP production, basal and FCCP-coupled OCR was significantly reduced in rapamycin treated LTS-derived fibroblasts.

3.4 Discussion

The results of this *in vitro* study suggest Rapamycin as a potentially new anti-fibroblast therapy for LTS. As shown, we observed a decrease in LTS fibroblast proliferation, function, and metabolism with rapamycin. High dose rapamycin demonstrated a significant reduction in every outcome measured as compared to vehicle medium and normal medium controls in the cells from the 5 patients included in this study. The results in these 5 LTS patients are supported by rapamycin's effect on fibroblasts in other organ systems including the lung, liver, and skin by decreasing expression and deposition of collagen type I and reducing cell proliferation. [26] [27] [47] This study suggests at a potential mechanism by assessing cellular respiration in LTS fibroblasts, which showed a reduced mitochondrial metabolic rate after treatment with rapamycin.

Bioenergetic analysis is a novel technique that monitors the oxygen consumption and extracellular acidification at a cellular level. [40] [48] [49] The key parameters of basal respiration, ATP production, and respiratory capacity may be measured to assess mitochondrial metabolism. [40] [49] Importantly, maximal respiratory capacity was significantly reduced in rapamycin-treated fibroblasts when non-mitochondrial respiration levels were normalized between control and rapamycin-treated groups. As seen in this study, the decreased basal respiration decreased ATP production, and maximal respiratory capacity after treatment suggests that rapamycin interferes with mitochondrial energy production resulting in decreased fibroblast function and collagen proliferation.

In clinical application for the treatment of LTS we expect rapamycin to exert an immunosuppressive effect in addition to antiproliferative effects. Rapamycin has FDA approval for immunosuppression to prevent rejection in renal transplant patients and is used to coat coronary stents to reduce inflammation and collagen synthesis. [50] [51] Furthermore, rapamycin was shown to disrupt mTOR signaling in fibroblasts and macrophages and reduce kidney fibrosis. [25] Therefore, we are encouraged by the potential of rapamycin treatment as adjuvant therapy for LTS. Modulating the immune response may be more effective than current medical therapies. In topical application, rapamycin could assist in suppressing the inflammatory response and fibroblast proliferation and collagen synthesis seen in LTS while avoiding side effects seen with systemic therapy. Ultimately, a rapamycin-eluting stent could direct sustained local immunotherapy and anti-fibroblast effect at the area of fibrosis while providing mechanical forces on the tracheal wall. Further in vivo investigation is required to support our data and hypothesis.

It is an in vitro study of human cells and the behavior of the LTS fibroblasts on culture dishes may not be representative of cells in vivo. While only passage 2 and 3 cells were used in experiments, the repeated passaging and freeze-thawing may have an effect on cell phenotype. Lastly, it is important to note that there was variability among LTS fibroblasts in the five different patients (**Figures 7A**, **8A**, **10A**, and **11D**) with varying response to rapamycin appreciated. This patient-specific variability in therapeutic response may be encountered with any clinical treatment and may be due to the heterogeneity of the disease process or possibly genetic differences in wound healing.

We are encouraged by the significant anti-fibroblast effect of rapamycin when the results from the five patients with LTS were averaged.

In summary, rapamycin demonstrated an anti-fibroblast effect by reducing the proliferation, metabolism, and collagen deposition of human LTS fibroblast *in vitro*. The bioenergetic effects of rapamycin demonstrated a significant decrease in oxidative phosphorylation of LTS fibroblasts, suggesting at a potential mechanism for the reduced proliferation and differentiation. Rapamycin's anti-fibroblast effects combined with its immunosuppressive action suggest at a promising adjuvant therapy for the treatment of laryngotracheal stenosis. Further studies are underway to compare the metabolism of normal and scar fibroblasts isolated from patients with LTS as well as to assess rapamycin's effect on laryngotracheal stenosis in an *in vivo* model.

CHAPTER 4 – RAPAMYCIN AS A TREATMENT FOR LARYNGOTRACHEAL STENOSIS USING MURINE MODEL *IN VIVO*

4.1 Introduction

The aim of this study is to address the *in vivo* effects of systemic rapamycin in a chemo-mechanical LTS murine model. Outcome measures include lamina propria thickness measurements of histological cuts from sacrificed animals, analysis of gene expression through RT-PCR, and post-operative weight and survival studies. The promise of rapamycin *in vivo* opens the potential for use in humans studies and eventually, as a potential therapy in the treatment of LTS. [4]

4.2 Materials and Methods

4.2.1 Experimental Design

This study was approved by the Johns Hopkins University Animal Care and Use Committee (MO12M354). 60 10-week old, male C57BL/6 mice (Charles River Laboratory) were used in this study. Surgery was performed in groups of thirty. Mice were sedated via an intraperitoneal (IP) injection of ketamine at a concentration of 100 mg/kg, and xylazine at a concentration of 10 mg/kg, prior to bleomycin coated wire-brush injury to the larynx and trachea to induce chemo-mechanical laryngotracheal stenosis (LTS). [4] Post-operatively, the thirty mice were divided into three cohorts of 10. Each cohort received an IP injection of 100μl of their assigned drug therapy. Our cohorts received either dexamethasone (Sigma-Aldrich, St. Louis, MO) at a concentration of 1 mg/kg, rapamycin (LC Labs, Woburn, MA) at a concentration of 4 mg/kg or phosphate buffered solution (PBS; Gibco Life Technologies by Invitrogen,

Grand Island, NY), once at the time of surgery, and then once every 48 hours, up until the 24 hours before sacrifice.

Each group of thirty mice was pre-designated to be either a one-week, two-week or three week cohort. Mice were sacrificed at the appropriate time point, and laryngotracheal complexes were dissected out in all groups for histologic analysis or RNA extraction for RT-PCR. Peri-operative and post-operative death rates were recorded throughout each group, with peri-operative deaths including mice deaths in the first 24 hours post-operatively. Our study concluded once we obtained seven specimens for each time point and treatment for histological analysis, and three specimens for each time point and treatment for RT-PCR. (**Figure 12**).

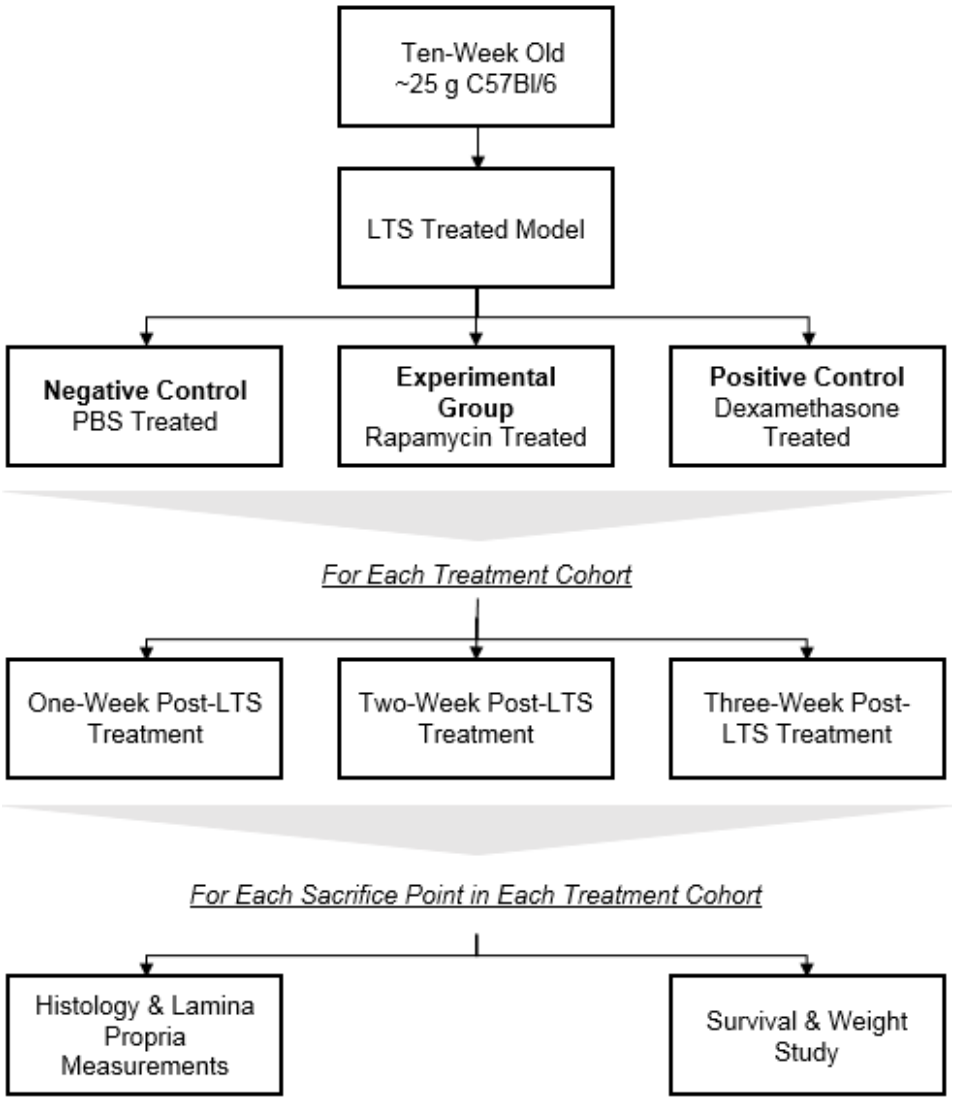

Figure 12 - Experimental Design

Flow chart of the in vivo experiments for rapamycin as a treatment for LTS in murine model

4.2.2 Histologic Measure Outcome

The primary outcome measure of this study is lamina propria (LP) thickness. Laryngotracheal complexes from each specimen were fixed in 10% formalin, and sent to the surgical pathology lab to be embedded in paraffin blocks. Slides were made from 5-μm-thick sections cut in the axial plane, which were then stained with hematoxiylin-eosin. Images were taken of these specimens at 5x magnification, and each specimen was assessed to measure LP thickness. Each specimen was split into 5 equal segments, and the thickest portion of each segment was measured and recorded. Measurements were performed from the medial aspect of the tracheal cartilage to the basement membrane of the epithelium. Assessment of all images was performed in a blinded fashion. Means and standard deviations were calculated from these results.

4.2.3 Mice Weight Outcome

A secondary outcome measure of this study is mice weight changes. Mice weights were recorded prior to surgery, at the time of every injection, and prior to sacrifice.

4.2.4 Statistical Analysis

Statistical significance for lamina propria thickness between groups was determined by the Mann-Whitney-Wilcoxon test and defined as $P < 0.05$. Weight data used a 2-way ANOVA test followed by a Tukey test for multiple comparisons and $P < 0.05$ was defined as significant.

4.3 Results

4.3.1 Measurable Increase in LP Thickness Following Chemomechanical Injury

Both rapamycin and dexamethasone intraperitoneal injection at one week demonstrate significant differences in lamina propria thickness versus the control group at p-value = 0.0012 and p-value = 0.0001, respectively (**Figure 13**).

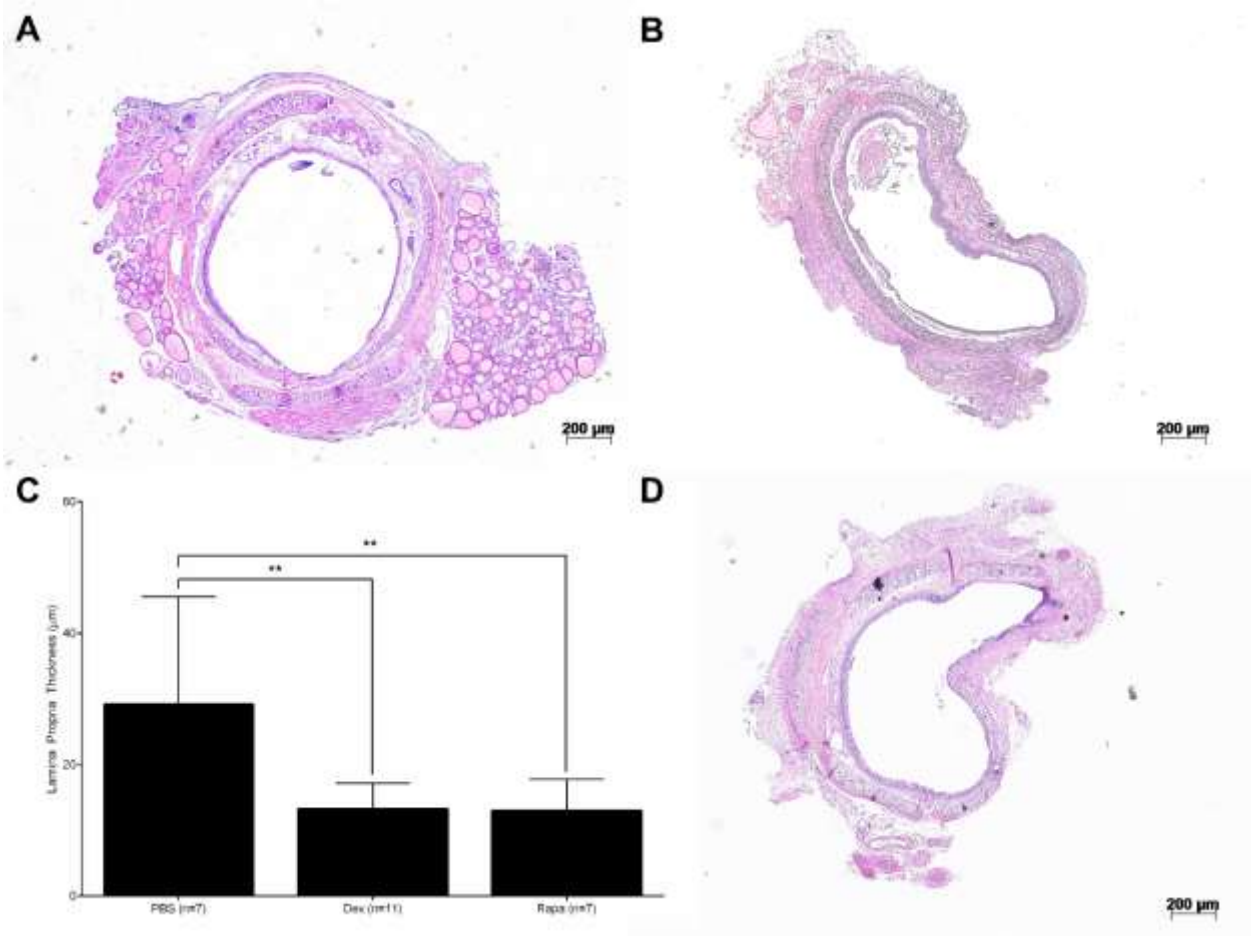

Figure 13 - Lamina Propria thickening

(A) Lamina propria thickness of PBS IP-injected animals, seven days post-operation (B) Lamina propria thickness of dexamethasone IP-injected animals, seven days post-operation (C) Lamina propria thickness quantification across all animals at seven days post-operation (D) Lamina propria thickness of rapamycin IP-injected animals, seven days post-operation

4.3.2 Survival and Weight Study for three weeks

At various injections points, weight measurements were recorded per the aforementioned methods. **Figure 14** shows the changes in weights over the various time points. Although of the surviving animals by the end of three weeks, the animals on average have recovered their weight, rapamycin and dexamethasone shows significant weight recovery from day six through day 16 post-operation when compared to PBS treated animals. **Table 1** demonstrates the significance of each time point.

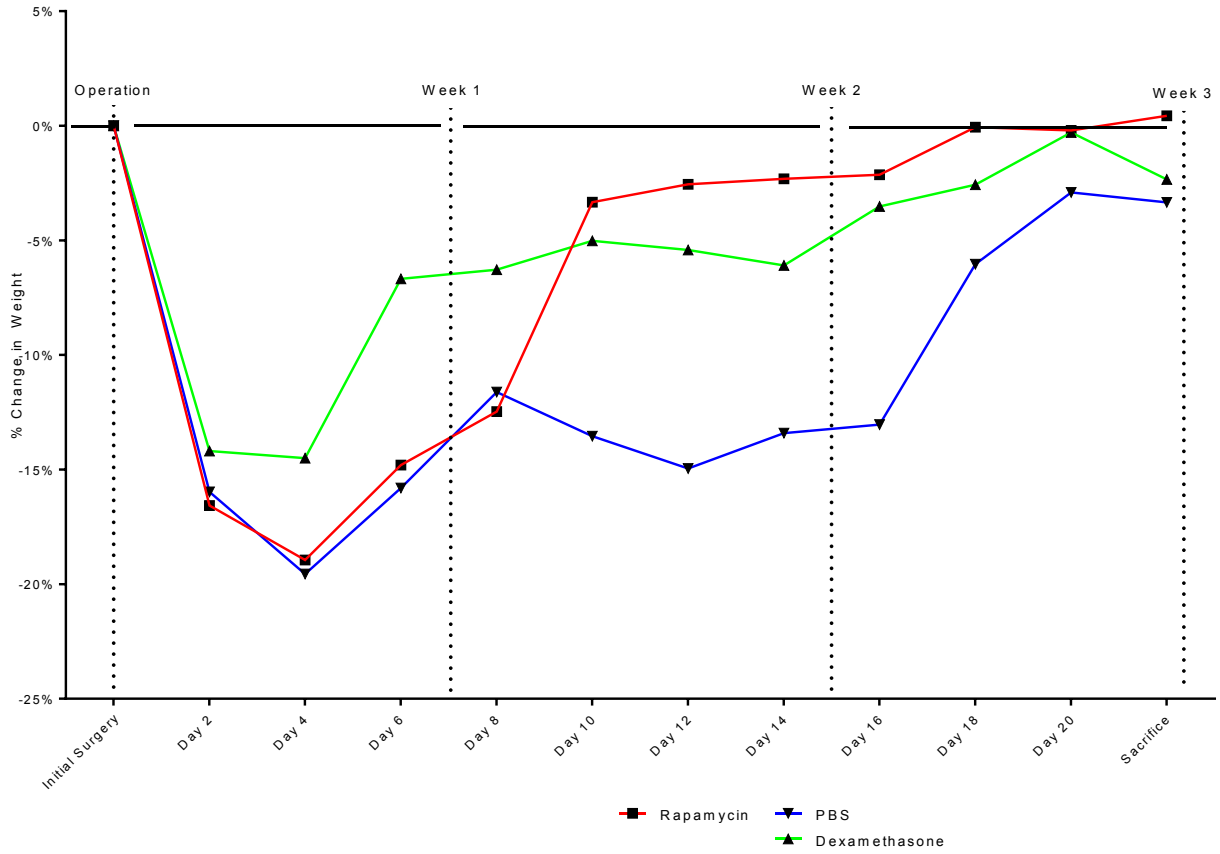

Figure 14 - Percent Weight Recovery Post-Operation

Rapamycin and dexamethasone demonstrate greater recover post-LTS operation when compared to PBS. Both drugs when injected IP are able to almost see full weight recovery by two weeks post-operation.

Table 1 - Significance values across injection time points for weight recovery

Test Variables	Mean Diff.	95% CI of diff.	Summary	Adjusted P Value
Initial Surgery				
PBS vs. Rapamycin	0	-5.786 to 5.786	ns	> 0.9999
PBS vs. Dexamethasone	0	-5.691 to 5.691	ns	> 0.9999
Day 2				
PBS vs. Rapamycin	0.6	-5.186 to 6.386	ns	0.9618
PBS vs. Dexamethasone	-1.78	-7.471 to 3.911	ns	0.7094
Day 4				
PBS vs. Rapamycin	-0.61	-6.658 to 5.438	ns	0.9638
PBS vs. Dexamethasone	-5.06	-11.00 to 0.8809	ns	0.1066
Day 6				
PBS vs. Rapamycin	-1.01	-8.128 to 6.108	ns	0.9299
PBS vs. Dexamethasone	-9.13	-16.25 to -2.012	**	0.009
Day 8				
PBS vs. Rapamycin	0.85	-7.202 to 8.902	ns	0.9604
PBS vs. Dexamethasone	-5.34	-13.22 to 2.538	ns	0.2287
Day 10				
PBS vs. Rapamycin	-10.21	-18.48 to -1.940	*	0.0124
PBS vs. Dexamethasone	-8.52	-16.57 to -0.4681	*	0.0362
Day 12				
PBS vs. Rapamycin	-12.4	-20.67 to -4.130	**	0.0019
PBS vs. Dexamethasone	-9.53	-17.80 to -1.260	*	0.0207
Day 14				
PBS vs. Rapamycin	-11.1	-19.37 to -2.830	**	0.006
PBS vs. Dexamethasone	-7.32	-15.59 to 0.9502	ns	0.0907
Day 16				
PBS vs. Rapamycin	-10.9	-19.17 to -2.630	**	0.0071
PBS vs. Dexamethasone	-9.52	-17.79 to -1.250	*	0.0209
Day 18				
PBS vs. Rapamycin	-5.98	-14.83 to 2.873	ns	0.2309
PBS vs. Dexamethasone	-3.47	-12.32 to 5.383	ns	0.5886
Day 20				
PBS vs. Rapamycin	-2.71	-12.46 to 7.036	ns	0.7609
PBS vs. Dexamethasone	-2.62	-12.37 to 7.126	ns	0.7742
Sacrifice				
PBS vs. Rapamycin	-3.78	-13.53 to 5.966	ns	0.595
PBS vs. Dexamethasone	-1	-10.75 to 8.746	ns	0.9626

4.3.3 Survival Study

Figure 15 shows peri-operative and post-operative deaths for the negative and positive control as well as the experimental group. Rapamycin and dexamethasone demonstrated higher survivability ($p = 0.531$, $p = 0.226$, respectively) when compared to the negative control, PBS IP-injection.

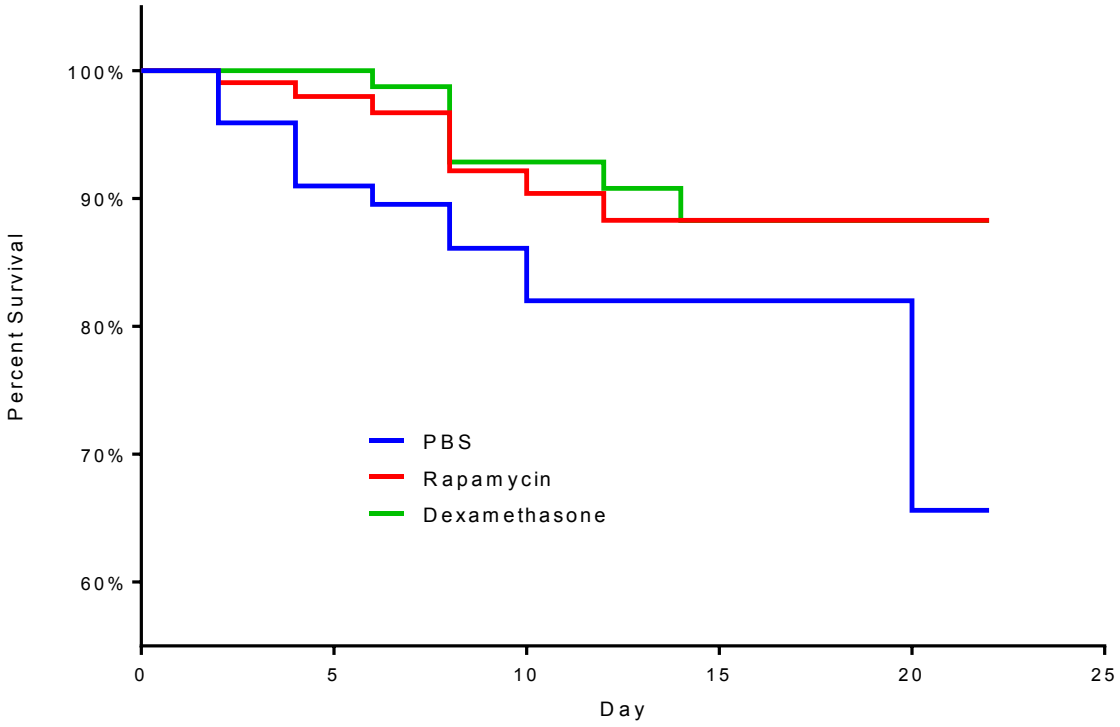

Figure 15 - Percent Survival by Time Point

As a percent of the initial animal count, the percent survival is the total number of animals survived over the total number of animals per condition.

4.4 Discussion

The evaluation of rapamycin in vivo for use in the treatment of Laryngotracheal stenosis is critical due to the inability of current treatments to limit the increasingly pervasive spread of the disease. From the analysis, we have determined that systemic rapamycin demonstrates a decrease in lamina propria thickness when compared to untreated cohort in a chemo-mechanical LTS murine model, an increased and quickened weight recovery in the chemo-mechanical LTS model compared to untreated cohort, and additional survivability.

The translatability of rapamycin to human possibilities is key to the introduction of this treatment from benchtop to bedside. Rapamycin is already used as anti-rejection medication for organ transplant and is also used on drug eluting stents throughout the body to prevent occlusion. Albeit, a systemic dosage or a more localized release of rapamycin via a drug-eluting stent, fundamentally rapamycin is an FDA-approved drug that has already showed its versatility. The treatment of LTS is merely another use amongst the plethora of current indications of the drug.

Although we understand that these results are very promising and may soon be used in the treatment of LTS in human patients. It is important to realize the limitations of the study. First, the use of an LTS murine model via chemo-mechanical introduction of LTS may not reflect the actual disease progress of LTS in humans. In addition, the animal model reflects particular aspects of the disease that may not necessarily be reflective in human patients. In addition, LTS manifests itself in patients due to various reasons,

cancer, prolonged intubation, including idiopathic pathologies. In order to confirm the usefulness of rapamycin, it would need to be used in clinical trials. Nevertheless, the ability of rapamycin *in vivo* to limit the progression and even treatment of LTS in the animal model shows promise that LTS may be an increasingly manageable disease.

CHAPTER 5 – CONCLUSIONS

5.1 Impact of Research

Laryngotracheal stenosis is a disease with no elegant solution. Physical methods using tracheostomy, stents, endoscopic scar excision and dilation, and tracheal & cricotracheal resection; [8] [9] [10] or use of cocktails of drugs including antibiotics and anti-inflammatory agents, have been commonly used to suppress stenosis. However, a valid method to tackle the source of the stenosis, on the fibrosis level has yet to come to light. The study on rapamycin, an FDA approved drug that is commonly used already on drug-eluting stents and as an anti-rejection agent, provides an effective means to decrease the proliferation of fibroblasts and subsequently cause animals with LTS to recover weight and decrease lamina propria thickness, both indicators for reduced LTS.

In conjunction with the use of rapamycin, understanding the Warburg-like difference between normal and fibrotic laryngotracheal fibroblasts is key to exploiting the metabolic difference. The analysis of normal and scar laryngotracheal fibroblasts illustrate proliferative, genetic and metabolic differences which can provides information on a more targeted approach to find a sustainable treatment for LTS. Understanding the difference between the two functional types of cells in the tracheal during LTS allows the research community a better perspective on how to treat the disease. Thus, this serves as a key to effectively treating this socially, physically and emotionally detrimental disease.

5.2 Future Directions

Continued analysis of the Warburg-like effect using additional HNSCC cell lines, an increased genetic panel, and additional patients would be necessary to examine and elucidate the greater connection between fibrosis of the trachea and cancer. Though it is important to understand the difference between normal and fibrotic fibroblasts, it's perhaps more critical to understand the variations between tracheal cancer and fibrosis. From this approach new drugs, therapies that were once unused for the treatment of LTS maybe more carefully selected. This could be a method to discover more effective treatments for LTS.

For rapamycin, beyond *in vivo* modeling of the drug to decrease LTS, human trials would be necessary to determine the actual validity of the hypothesis that LTS can be treated with rapamycin. The genetic variability in humans could alter the effects of the drug and its efficacy at treating LTS. Oral dosage of rapamycin both in the short term and the long term should be used and compared against a control group to see whether or not patients demonstrate decreased stenosis. Pending significant results, it would be useful to explore less systemic methods of rapamycin delivery. Given that rapamycin is already used in drug-eluting students for the artery, this could be translated to drug eluting stents for the trachea. The stent provides a physical barrier against LTS thickening and also delivers localized rapamycin to suppress fibroblast proliferation. These methodologies, given strong data, can be more effective treatments to this crippling disease.

REFERENCES

[1] H. C. Herrington, S. M. Weber and P. E. Andersen, "Modern Management of Laryngotracheal Stenosis," *The Laryngoscope,* vol. 116, pp. 1553-1556, September 2006.

[2] M. Jette, S. Hayer and S. Thibeault, "Characterization of human vocal fold fibroblasts derived from chronic scar," *Laryngoscope,* vol. 123, no. 3, pp. 738-745, 3 2013.

[3] G. Halmos, F. Schuiringa, D. Palinko and e. al., "Finding balance between minimally invasive surgery and laryngotracheal resection in the management of adult laryngotracheal stenosis," *Eur Arch Otorhinolaryngol,* vol. 271, pp. 1967-1971, 2014.

[4] A. Hillel, D. Namba, D. Ding, V. Pandian, J. Elisseeff and M. R. Horton, "An In Situ, In Vivo Murine Model for the Study of Laryngotracheal Stenosis," *JAMA Otolaryngology–Head & Neck Surgery,* vol. 140, no. 10, 2014.

[5] A. Ghosh, N. Malaisrie, K. Leahy, S. Singhal, E. Einhorn, P. Howlett, N. A. Cohen and N. Mirza, "Cellular Adaptive Infammation Mediates Airway Granulation in a Murine Model of Subglottic Stenosis," *Otolaryngology - Head and Neck Surgery,* vol. 144, no. 6, pp. 927-933, 2011.

[6] B. Minnigerode and H. Richter, "Pathophysiology of subglottic tracheal stenosis in childhood," *Treachea and Lung Surgery in Childhood,* pp. 1-7, 1987.

[7] A. Hillel, H. 3. Johns, E. Hapner, M. Shah, J. Wise and A. Klein, "Voice outcomes from subligamentous cordectomy for early glottic cancer," *The Annals of Otology, Rhinology, and Laryngology,* vol. 122, no. 3, pp. 190-196, 2013.

[8] R. Cotton, "Pediatric Laryngotracheal Stenosis," *J Pediatr Surg,* vol. 19, pp. 699-704, 1984.

[9] A. F. Hseu, M. S. Benniger, T. M. Haffey and R. Lorenz, "Subglottic Stenosis: A Ten-Year Review of Treament Outcomes," *The Laryngoscope,* vol. 124, pp. 736-741, March 2014.

[10] D. E. Schuller, "Long-term stenting for laryngotracheal stenosis," *Annals of Otology, Rhinology & Laryngology,* vol. 89, no. 6, pp. 515-520, 1980.

[11] A. Ghosh, G. Philiponis, J. Lee and e. al, "Pulse steroid therapy inhibits murine subglottic granulation," *Otolaryngol Head Neck Surg,* vol. 148, pp. 284-290, 2013.

[12] C. Croft, K. Zub and B. Borowiecki, "Therapy of iatrogenic subglottic stenosis: a steroid/antibiotic regimen," *The Laryngoscope,* vol. 148, pp. 284-290, 1979.

[13] N. Li, F. Chen, F. Dikkers and e. al, "Dose-dependent effect of mitomycin C on human vocal fold fibroblasts," *Head Neck,* vol. 36, pp. 401-410, 2014.

[14] J. Supance, "Antibiotics and steroids in the treatment of acquired subglottic stenosis: A Canine Model Study," *Annals of Otology, Rhinology & Laryngology,* vol. 92, no. 4, pp. 377-382, 1983.

[15] J.-L. Roh, L. Yong-Won and P. Chan, "Can mitomycin C really prevent airway stenosis," *The Laryngoscope,* vol. 116, no. 3, pp. 440-445, 2006.

[16] J.-L. Roh, "Prevention of posterior glottic stenosis by mitomycin C," *Annals of Otology, Rhinology & Laryngology,* vol. 114, no. 7, pp. 558-562.

[17] D. R. Namba, G. Ma, I. Samad, D. Ding, V. Pandian, J. D. Powell, M. R. Horton and A. T. Hillel, "Rapamycin inhibits Human Laryngotracheal Stenosis-derived fibroblast Proliferation, Metabolism, and Function In Vitro," *American Academy of Otolaryngology-Head and Neck Surgery,* vol. Accepted, 3 2015.

[18] H. Kil, M. Alberts and e. a. Liggitt HD, "Dexamethasone treatment does not ameliorate subglottic ischemic injury in rabbits," *Chest,* vol. 111, pp. 1356-1360, 1997.

[19] M. Cardenas and J. Heitman, "FKBP12-rapamycin target TOR2 is a vacuolar protein with an associated phosphatidylinositol-4 kinase activity," *EMBO J,* vol. 14, pp. 5892-5907, 1995.

[20] E. Brown, M. Albers and T. Shin, "A mammalian protein targeted by G1-arresting rapamycin-receptor complex," *Nature,* vol. 369, pp. 756-758, 1994.

[21] D. Granger, J. Bromwell and S. Chen, "Prolongation of renal allograft survival in a large animal model by oral rapamycin monotherapy," *Transplantation,* vol. 59, pp. 183-186, 1995.

[22] R. Saunders, M. Metcalfe and M. Nicholson, "Rapamycin in Transplantation: a review of the evidence," *Kidney Int. ,* vol. 17, pp. 660-665, 2001.

[23] T. Suzuki, G. Kopia and S. Hayashi, "Stent-based delivery of sirolimus reduces neointimal formation in a procine coronary model," *Circulation,* vol. 104, pp. 1188-1193, 2001.

[24] M. Morice, P. Serruys and J. Sousa, "A randomized comparison of a sirolimus-eluating stent iwth a standard stent for coronary revasculariozation," *New England Journal of Medicine,* vol. 346, pp. 1773-1780, 2002.

[25] G. Chen, H. Chen and C. Wang, "Rapamycin ameliorates kidney fibrosis by inhibiting the activation of mTOR signaling in intestitial macrophages and myofibroblasts," *PLoS One,* vol. 7, 2012.

[26] Z. Tamaki, Y. Asano, M. Kubo and e. al., "Effects of the immunosuppressant rapamycin on the expression of human alpha2(I) collagen and matrix metalloproteinase 1 genes in scleroderma dermal fibroblasts," *Joural of Dermatological Science,* vol. 74, pp. 251-259, 2014.

[27] J. Zhu, J. Wu and E. Frizell, "Rapamycin inhibits hepatic stellate cell proliferation in vitro and limits fibrogenesis in and in vivo model of liver fibrosis," *Gastroenterology,* vol. 117, pp. 1198-1204, 1999.

[28] D. Blyth, T. Wharton, M. Pedrick, T. J. Savage and S. Sanjar, "Airway Subepithelial Fibrosis in a Murine Model of Atopic Asthma, Suppression by Dexamethasone or Anti–Interleukin-5 Antibody," *American Journal of Respiratory Cell and Molecular*

Biology, vol. 23, no. 2, pp. 241-246, 2000.

[29] B. Melgert, P. Olinga, J. M. Van Der Laan, B. Weert, J. Cho, D. Schuppan, G. M. Groothuis, D. Meijer and K. Poelstra, "Targeting dexamethasone to Kupffer cells: Effects on liver inflammation and fibrosis in rats," *Hepatology,* vol. 34, no. 4, pp. 719-728, 2001.

[30] W. Dik, R. McAnulty, B. Naber, L. Zimmermann, G. Laurent and S. Mutsaers, "Short course dexamethasone treatment following injury," *Thorax,* vol. 58, pp. 765-771, 2003.

[31] G. S. Hoffman, C. K. Thomas-Golbanov, J. Chan, L. M. Akst and I. Eliachar, "Treatment of subglottic stenosis, due to Wegener's granulomatosis, with intralesional corticosteroids and dilation," *The Journal of Rheumatology,* vol. 30, no. 5, pp. 1017-1021, 2003.

[32] D. Rockey, D. Bell and J. Hill, "Fibrosis - A common pathway to organ injury and failure," *The New England Journal of Medicine,* vol. 372, no. 12, pp. 1138-1149, 18 March 2015.

[33] S. S. Chang, W. W. Jiang, I. Smith, L. M. Poeta and e. al, "MicroRNA alterations in head and neck squamous cell carcinoma," *Int. J. Cancer,* vol. 123, no. 12, 2008.

[34] Invitrogen, "Quant-iT PicoGreen dsDNA Reagent and Kits," *Invitrogen,* pp. 1-7, 10 June 2008.

[35] C. Schneider, W. Rasband and K. Eliceiri, "NIH Image to ImageJ: 25 years of image analysis," *Nature Methods,* vol. 9, pp. 671-675, 28 June 2012.

[36] T. A. Valdez and S. M. Shapshay, "Idiopathic subglottic stenosis revisited," *Annals of Otology, Rhinology & Laryngology,* vol. 111, no. 8, pp. 690-695, 2002.

[37] M. G. Vander Heiden, L. C. Cantley and C. B. Thompson, "Understanding the Warburg Effect: The Metabolic Requirements of Cell Proliferation," *Science,* vol. 324, no. 5930, pp. 1029-1033, 22 May 2009.

[38] J.-w. Kim and C. V. Dang, "Cancer's molecular sweet tooth and the Warburg effect," *Cancer reserach,* vol. 66, no. 18, pp. 8927-8930, 2006.

[39] A. Hall, K. D. Meyle, M. K. Lange, M. Klima, M. Sanderhoff, C. Dahl, C. Abildgaard, K. Thorup, S. M. Moghimi, P. B. Jensen, J. Bartek, P. Guldberg and C. Christensen, "Dysfunctional oxidative phosphorylation makes malignant melanoma cells addicted to glycolysis driven by the V600EBRAF oncogene," *Oncotarget,* vol. 4, no. 4, pp. 584-599, 8 April 2013.

[40] M. D. Brand and D. G. Nicholls, "Assessing mitochondrial dysfunction in cells," *Biochemical Journal,* vol. 435, no. 2, pp. 297-312, 2011.

[41] J. S. Modica-Capolitano and K. K. Singh, "Mitochondrial dysfunction in cancer," *Mitochondrion,* vol. 4, no. 5, pp. 755-762, 2004.

[42] S. Ahn, J. Costa and J. Emanuel, "PicoGreen quantitation of DNA: effective evaluation of samples pre- or post-PCR," *Nucleic Acids Res,* vol. 24, pp. 2623-2625, 1996.

[43] A. Hillel, V. S, J. Petsche and e. al, "Embryonic germ cells are capable of adipogenic differentiation in vitro and in vivo," *Tissue Eng Part A,* vol. 15, pp. 479-186, 2009.

[44] K. Livak and T. Schmittgen, "Analysis of relative gene expression data using real-time quantitative PCR and the 2(-Delta delta C(T)) Method," *Methods,* vol. 25, pp. 402-408, 2001.

[45] A. Hillel, S. Untermam and Z. e. a. Nahas, "Photoactivated composite biomaterial for soft tissue restoration in rodents and in humans," *Sci Transl Med,* vol. 3, p. 93ra67, 2011.

[46] R. Schuh, P. Clerc and e. a. Hwang H, "Adaptation of microplate-based respirometry for hippocampal slices and analysis of respiratory capacity," *J Neurosci Res,* pp. 1979-1988, 2011.

[47] N. Poulalhon, F. D, N. Roos and e. al, "Modulation of collagen and MMP-1 gene expression in fibroblasts by the immunosuppressive drug rapamycin. A direct role as an antifibrotic agent?," *J Biol Chem,* vol. 281, pp. 33045-33052, 2006.

[48] J. Singh and S. Giri, "Loss of AMP-activated protein kinase in X-linked adrenoleukodystrophy patient-derived fibroblasts and lymphocytes," *Biochem Biophys Res Commun,* vol. 445, pp. 126-131, 2014.

[49] M. Wu, A. Neilson, A. Swift and e. al, "Multiparameter metabolic analysis reveals a close link between attenuated mitochondrial bioenergentic function and enhanced glycolysis dependency in human tumor cells," *Am J Physiol Cell Physiol,* vol. 292, pp. 126-136, 2007.

[50] S. Sehgal, "Rapamune (Sirolimus, rapamycin): an overview and mechanism of action.," *Ther Drug Monit,* vol. 17, pp. 660-665, 1995.

[51] M. Costa and D. Simon, "Molecular basis of restenosis and drug-eluting stents," *Circulation,* vol. 111, pp. 2257-2273, 2005.

CURRICULUM VITAE

Garret Ma

(208) 695-4397 • 2427 E. Gloucester Boise, Idaho 83706 • garretma@gmail.com

EDUCATION

Johns Hopkins University GPA 3.7 – *Thesis Based*
M.S.E Biomedical Engineering (Full Scholarship) *May 2015*

University of California at Los Angeles GPA 3.6 – *Cum Laude, Tau Beta Pi (Top 20%)*
B.S. Bioengineering, minor in Global Studies *Jun 2012*

RESEARCH EXPERIENCE

Johns Hopkins University | Department of Biomedical Engineering **Baltimore, MD**
Graduate Researcher with Dr. Jennifer Elisseeff & Dr. Alexander Hillel *Sep 2013 to Present*

Characterization and rapamycin treatment of laryngotracheal stenosis *in vitro* and evaluation of the efficacy and safety of the drug in a murine LTS model *in vivo*

- Hypothesized that Rapamycin induced human tracheal fibroblasts reduce cellular proliferation and metabolism, designed experiment to validate hypothesis and reported research results in publication in *Otolaryngology – Head & Neck Surgery*
- Characterized the significant metabolic, proliferative, morphological and genetic differences between normal and fibrotic laryngotracheal fibroblasts *in vitro*. Results in two submission.
- Determined the in vivo effects of rapamycin on a laryngotracheal stenosis murine model for outcomes in lamina propria thickness and weight/survival changes. Results in submission.

Evaluation of extracellular matrices (ECM) in vitro and in vivo particularly Chondroitin Sulfate N-hydroxysuccinimide and Acellular adipose extracellular matrices

- Investigated the mechanical properties of hydrogels form by crosslinking Chondroitin Sulfate with various extracellular matrices; research developed into a paper, in submission.
- Submitted Innovated New Drug to the Food & Drug Administration (FDA) to begin clinical trials of Acellular Adipose ECM. Acceptance, pending.

Department of Medicine | University of California at Los Angeles **Los Angeles, CA**
Undergraduate Researcher under Dr. Paul Krogstad *Sep 2011 to Jun 2012*

Modified backbone structure of picornavirus Coxsackievirus B3 plasmid by altering the internal ribosome entry site (IRES) and inserting a T7 promoter region to create a more effective and efficient method of modifying viruses

- Incorporated IRES of various known strains of Coxsackievirus and evaluated virulence and replication rates
- Transfected plasmid into HeLa cells, analyzed cytopathic effects and established viral titers via plaque assays

Department of Bioengineering | University of California at Los Angeles **Los Angeles, CA**
Undergraduate Researcher under Dr. James Dunn *Sep 2008 to Jun 2011*

Engineered novel methods to mechanically and chemically enhance nutrient absorption of rats suffering from surgically induced short bowel syndrome

- Mechanically expanded anastomotic jejunum of adult rats to increase villus and crypt surface area via spring force
- Enhanced vascularization of shortened ilium and jejunum with vascular endothelial growth factor (VEGF) thereby increasing surface area of nutrient absorption

- Established baseline enzymatic activity in unexpanded jejunum and compared villus and crypt lengths of unexpanded and expanded small bowel

Analyzed the effects of varying extracellular matrices and growth factors on the proliferation of primary interstitial cells of Cajal (ICC) from neonatal rats and mice

- Evaluated ICC calcium concentration fluctuation *in vitro* using fluo-4 acetoxymethyl ester Ca^{2+} indicators
- Established morphological indicators and metrics to qualitatively determine undifferentiated ICC growth

PUBLICATIONS

Namba, D. R., Ma, G., Samad, I., Ding, D., Pandian, V., Powell, J. D., ... & Hillel, A. T. (2015). Rapamycin Inhibits Human Laryngotracheal Stenosis-derived Fibroblast Proliferation, Metabolism, and Function in Vitro. Otolaryngology--head and neck surgery: official journal of American Academy of Otolaryngology-Head and Neck Surgery.

N.Y. Lei, G. Ma, T. Zupekan, R. Stark, M. Puder, and J.C.Y. Dunn, "Controlled release of vascular endothelial growth factor enhances intestinal adaptation in rats with extensive small intestinal resection," *Surgery* **150**(2): 186-190, 2011.

PRESENTATIONS

G. Ma, J. Yang, M. Wong, M. Ngai, L. Sharpe and J. Reed, "Microfluidic device for routine, high-resolution expression profiling of clinical biopsies and single cells", Podium and Poster Presentations at the UCLA Bioengineering Symposium, Los Angeles, California, March 2012.

N.Y. Lei, G. Ma, T. Zupekan, R. Stark, M. Puder, and J.C.Y. Dunn, "Controlled release of vascular endothelial growth factor enhances intestinal adaptation in rats with extensive small intestinal resection", Podium Presentation at the 6th Annual Academic Surgical Congress, Huntington Beach, California, February 2011.

INDUSTRY EXPERIENCE

Bain & Company **San Francisco, CA**
Associate Consultant Oct 2015 (start date)

Abbott Fund | LifeNet International **Bujumbura, Burundi, East Africa**
Consultant *Jan 2013 to Aug 2013*

- Optimized and reorganized pharmaceutical deliveries to upcountry clinics by 10-fold from 6 to 60 rural clinics and hospitals
- Automated ordering and pricing model with Visual Basic that reduced order processing time by 75% and drug costs by 5%

Abbott Laboratories | Vascular **Temecula, CA**
Quality Engineer for Endovascular Stents *Jun 2012 to Dec 2012*

- Managed technicians from three stent production lines to evaluate risk of defects and examine quality of stents in production
- Raised >$20k for Abbott Employee Giving Campaign as the divisional campaign organizer for 200+ employees

Abbott Laboratories | Global Pharmaceutical Operations **Waukegan, IL**
Quality Engineer Intern focused on Proprietary Pharmaceutical Products *Jun 2011 to Sep 2011*

- Developed program written in Visual Basic that streamlined pharmaceutical trend monitoring process by 38%

- Designed program that improved database extraction efficiency and reduced dataset building times by 67%

LEADERSHIP

Discovery 2 Market | Carey Business School **Johns Hopkins University**
Scientific Advisor *Feb 2015 to Present*

- Advises seven global MBA students at JHU Carey Business School on scientific issues associated with Chondroitin Sulfate in a capacity ranging from Innovative New Drug submissions, business licensing, market sizing/share and various scientific concepts associated with them product.

Graduate Representative Organization **Johns Hopkins University**
Treasurer *Sep 2013 to Present*

- Facilitated and allocated around $175k budget that was distributed among 20+ events and clubs across the graduate community.

Johns Hopkins Graduate & Consulting Club **Johns Hopkins University**
Competitor *Sep 2013 to Present*

- Finalist among 60 teams in JHBCC Biotechnology Case Competition held in April 2014; Finalist among 67 teams in JHBCC Mini-Case Competition in November 2013; Winner among 10 teams in the Deloitte Case Competition held in September 2013

Biomedical Engineering Society **University of California at Los Angeles**
President *Sep 2011 to Jun 2012*

- Led meetings of 30+ board members covering budget, event planning and marketing strategies
- Promoted a community atmosphere for the students in the Department of Bioengineering
- Coordinated *Science Vendor Exposition* to bring scientific equipment vendors to UCLA at a discounted price
- Connected Biomedical Engineering Society with numerous biotech and pharmaceutical companies in LA-metro area

Tau Beta Pi, California Epsilon **University of California at Los Angeles**
Biomedical Engineering Society Club Liaison *Jan 2012 to June 2012*

- Tutored underclassman in engineering subjects including bioengineering, physics, chemistry, and calculus
- Coordinated events between local UCLA chapters of Tau Beta Pi and Biomedical Engineering Society
- Volunteered in an after school program teaching physics at a local low income elementary school

Department of Medicine **University of California at Los Angeles**
Lecturer *Sept 2010 to June 2011*

- Taught a college course entitled "*AIDS in Sub-Saharan Africa: A Modern Plague*" at UCLA for class of 20+ students
- Prepared lectures and facilitated discussions on the economic, political and social impact of HIV prevalence
- Organized guest lectures from leaders in the Global Health Field at UCLA to touch on various topics including HIV

HONORS AND AWARDS

Tau Beta Pi, California Epsilon (Initiated 2010)
National Engineering Honor Society for engineering students with strong academic achievement (Top 1/5 of Class)

A.V. Balakrishnan Scholar for Academic Excellence (2012)
UCLA Engineering scholarship for students that demonstrate exceptional academic and research excellence

Engineering Award for Student Welfare (2012)
Award for outstanding contributions to student welfare through participation in extracurricular activities and who have given outstanding service to the campus community

Dean's List (Awarded four times from 2008-2012)
Award for students that maintain a 3.70 or above Grade Point Average in a single quarter